

A redescription of the three longest-known species of the acanthodian *Cheiracanthus* from the Middle Devonian of Scotland

Carole Burrow, Jan den Blaauwen, and Michael Newman

ABSTRACT

The cheiracanthid acanthodiforms were widespread during the Middle Devonian, often being the most abundant acanthodians in northern European vertebrate macro- and microfaunal assemblages. Three species of cheiracanthids, *Cheiracanthus murchisoni*, *C. grandispinus*, and *C. latus*, have been known from the Middle Devonian (Eifelian–Givetian) of northern Scotland since the nineteenth century. Here we review the anatomy of these species and show that the main distinguishing features for the three species are the scale ornamentation, general body shape, and relative robustness of their scapulocoracoids and fin spines. They also show different stratigraphic and geographic distributions in the Orcadian Basin. All three species appear at the base of the *Coccosteus cuspidatus* + *Pterichthyodes milleri* placoderm biostratigraphic zone; *C. latus* disappears towards the upper limit of this zone, *C. murchisoni* extends into the base of the overlying *Dickosteus threiplandi* zone, and *C. grandispinus* reaches up to the middle of this zone. Some cheiracanthid taxa based on isolated scales from the Baltic countries, Belarus, and Russia are considered junior synonyms of the Scottish species. The new data we provide should prove helpful in further elucidating the taxonomic position of cheiracanthids.

Carole Burrow. Geosciences, Queensland Museum, 122 Gerler Rd, Hendra, Brisbane, Queensland 4011, Australia. carole.burrow@gmail.com

Jan den Blaauwen. University of Amsterdam, Science Park 904, 1098 XH, Amsterdam, Netherlands. J.L.denBlaauwen@uva.nl

Michael Newman. Vine Lodge, Vine Road, Johnston, Haverfordwest, Pembrokeshire, SA62 3NZ, United Kingdom. ichthyman5@gmail.com

Keywords: *Cheiracanthus*; Orcadian Basin; histology; biostratigraphy; Orkney; Moray Firth; Caithness

Submission: 26 September 2019. Acceptance: 25 March 2020.

INTRODUCTION

The Cheiracanthidae are a family of acanthodiform acanthodians that we consider to be represented by two genera based on articulated fish, *Cheiracanthus* and *Homalacanthus*; another genus, *Markacanthus*, is known only from isolated scales (Valiukevičius, 1985). *Cheiracanthus* spp. were abundant in Middle Devonian vertebrate faunal assemblages of northern Europe, with isolated scales described from the Baltic countries and Russia (e.g., Gross, 1973; Valiukevičius, 1985, 1988; Glinskiy and Pinakhina, 2018; Pinakhina, 2018; Pinakhina and Märss, 2018), and articulated fish from Scotland and Spitsbergen (Agassiz, 1835; Egerton, 1861; McCoy, 1848; Newman et al., 2019). Only one valid new species based on articulated specimens, *C. peachi* den Blaauwen, Newman and Burrow, 2019, from Scotland, has been described since the nineteenth century. Rare scales have been recorded from Greenland (Blom et al., 2006) which are now recognised as *C. intricatus* Valiukevičius, 1985, but records of *Cheiracanthus* from elsewhere in the world are now considered incorrect or dubious: scales from Antarctica described by White (1968) were subsequently assigned to the diplacanthid *Milesacanthus antarctica* Young and Burrow, 2004, and *Cheiracanthus? costellatus* Traquair, 1893, from the Emsian of eastern Canada is most likely a diplacanthiform (CJB personal observation). The only other cheiracanthid genus is *Homalacanthus* Russell, 1951, with the type and only valid species being *H. concinnus* (Whiteaves, 1887) from the Frasnian of Quebec. Miles (1966) also assigned *Protogonacanthus* and *Carycinacanthus* to the Cheiracanthidae, but we consider them to be acanthodids, based on their unornamented scale crowns; also, *Carycinacanthus* is now considered to be a junior synonym of *Acanthodes* (Beznosov 2009). Miles (1966) and Denison (1979) considered the cheiracanthids to be a grade within the Family Acanthodidae, but we maintain Berg's (1940) classification, with the Cheiracanthidae being a Family within the order Acanthodiformes based on their endoskeletal structure and scale ornament (Burrow and den Blaauwen, in press).

The only other cheiracanthid known from articulated fish is *Homalacanthus* Russell, 1951, with the type and only valid species being *H. concinnus* (Whiteaves, 1887) from the Frasnian of Quebec. Miles (1966) also assigned *Protogonacanthus* and *Carycinacanthus* to the Cheiracanthidae, but we consider them to be acanthodids,

based on their unornamented scale crowns; also, *Carycinacanthus* is now considered to be a junior synonym of *Acanthodes* (Beznosov, 2009). Miles (1966) and Denison (1979) considered the cheiracanthids to be a grade within the Family Acanthodidae, but we maintain Berg's (1940) classification, with the Cheiracanthidae being a Family within the order Acanthodiformes based on their endoskeletal structure and scale ornament (Burrow and den Blaauwen in press). Recent phylogenetic analyses often show cheiracanthids (i.e. *Cheiracanthus* and *Homalacanthus*) as paraphyletic with respect to *Acanthodes* (e.g. Burrow et al., 2016; Coates et al., 2018), but their character matrices did not code specifically for the type of mineralised tissue forming the jaw cartilages, or for ornamented vs. smooth scale crowns. Older analyses of selected mid-Palaeozoic acanthodians focussing on the group interrelationships (Hanke and Wilson, 2004; Burrow and Turner, 2010) showed *Homalacanthus* and *Cheiracanthus* as sister taxa, but these analyses omitted the Permian *Acanthodes*.

Here we provide detailed descriptions of the general anatomy and morphology and histology of dermal elements and endoskeleton of the three valid Scottish Middle Devonian *Cheiracanthus* spp. erected in the nineteenth century, and discuss their biostratigraphical and biogeographical distribution. Institutional abbreviations: MHNN FOS, Neuchâtel Natural History Museum; NHMUK, Natural History Museum, London; NMS, National Museums of Scotland; NMV, Museums Victoria, Melbourne; NRM, Natural History Museum of Sweden, Stockholm; USCP, University of Sheffield Centre for Palaeontology; SM, Sedgwick Museum, Cambridge.

HISTORY OF RESEARCH ON *CHEIRACANTHUS* FROM SCOTLAND

Cheiracanthus murchisoni Agassiz, 1835

Cheiracanthus murchisoni was one of the first Devonian fish to be described. It was erected by Agassiz based on IGUN.66 in the Neuchâtel Museum collection (now MHNN FOS39) from Gamrie (Agassiz 1833-1843, plate 1c, figure 3; Figure 1.1, 1.3). *Cheiracanthus minor* Agassiz, 1835 was erected in the same work, figuring one specimen (Agassiz 1833-1843, plate 1c, figure 5). This specimen was part of the Traill collection and is now considered lost (Andrews 1982). Miller (1841, plate 7, figure 1) figured a specimen of *Cheiracanthus* but did not give it a species name. Agassiz later erected *Cheiracanthus microlepidotus* Agas-

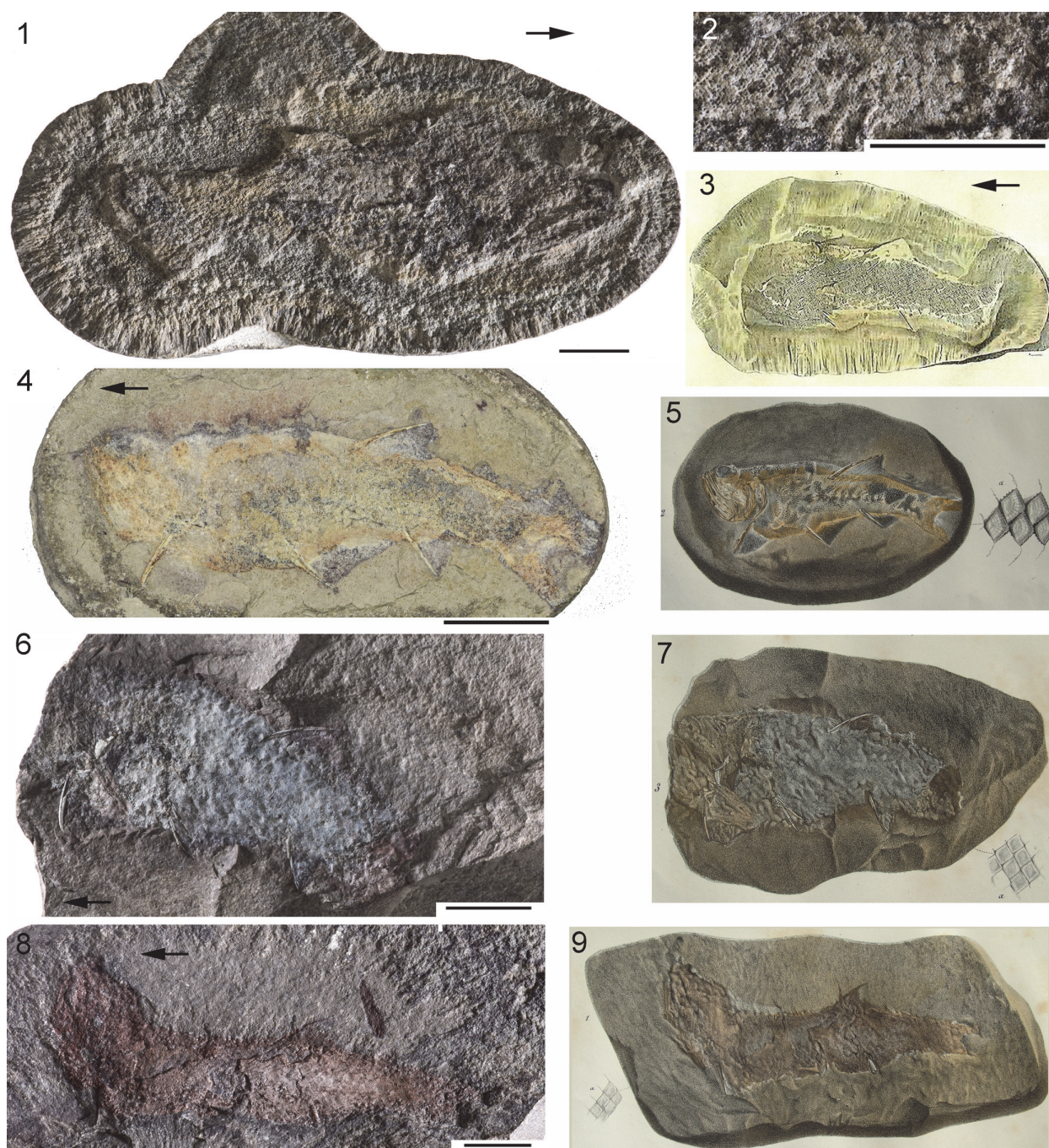


FIGURE 1. Type material of *Cheiracanthus murchisoni* Agassiz, 1835 and its junior synonym *C. microlepidotus* Agassiz, 1844. 1-3, Holotype MHNN FOS 39 from Gamrie: 1, specimen in present condition; 2, closeup of midbody scales; 3, image in Agassiz (1833-43, plate 1c, figure 3). 4-9: Syntypes of the junior synonym *C. microlepidotus* from Lethen Bar: 4, 5, NHMUK PV P544; 6, 7, MHNN FOS 40; 8, 9, MHNN FOS 41. Scale bars equal 20 mm.

siz, 1844 based on three specimens from Lethen Bar, NHMUK P.544 (Agassiz 1844-1845, plate 15, figure 2; Figure 1.4, 1.5), and MHNN FOS 40, 41 (Figure 1.6-9). Agassiz also produced a restoration of the genus (Agassiz 1844-1845, plate D, figure 2). Miller (1847) reproduced his *Cheiracanthus* fig-

ure from his earlier publication, but this time labelled it *Cheiracanthus microlepidotus*; NMS G.1953.4.2 is the specimen on which the figure was based. M'Coy (1848) erected two new species based on specimens from Orkney, *Cheiracanthus lateralis* M'Coy, 1848, and *Cheiracanthus pulveru-*

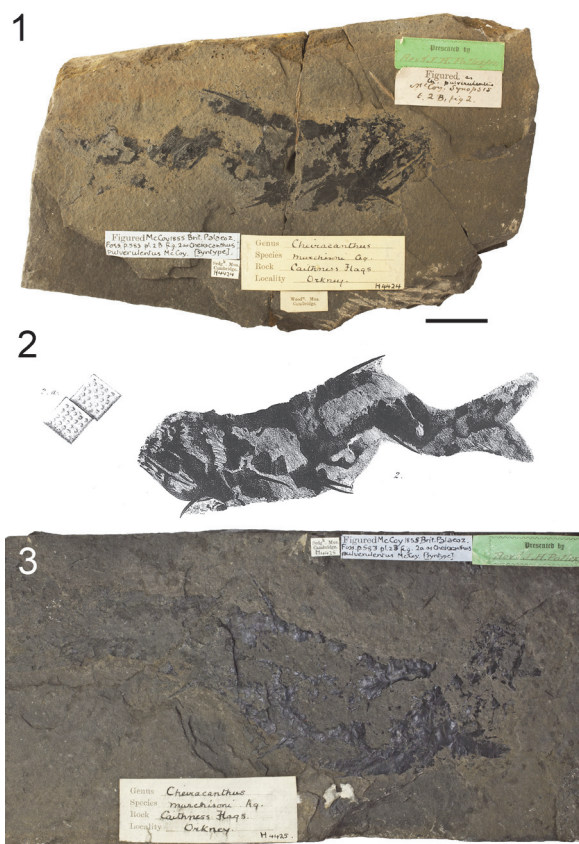


FIGURE 2. Syntypes of *Cheiracanthus pulverulentus* M'Coy, 1855 from Orkney, a junior synonym of *Cheiracanthus murchisoni*. 1, SM H4424, 'syntype' specimen in present condition; 2, SM H4424 specimen and scales as illustrated by M'Coy (1855, plate 2.B, figure 2), showing a mirror image of the specimen; 3, SM H4425, second 'syntype', present condition. Scale bars equal 20 mm.

lentus M'Coy, 1848, neither of which were figured. He later illustrated one of the *C. pulverulentus* syntypes SM H4424 (M'Coy 1855, plate 2.B, figure 2; Figure 2.1, 2.2; the other syntype is illustrated in Figure 2.3) and included a description of the other known species in that work.

Egerton (1860) considered *Cheiracanthus lateralis* a junior synonym of *Cheiracanthus minor* as there were no specific characters to separate them. Subsequently, Traquair (1888) considered that the character differences exhibited in *Cheiracanthus microlepidotus*, *Cheiracanthus minor* and *Cheiracanthus pulverulentus* resulted from the different preservation at the various localities, and united them [as well as *C. lateralis* which had already been dealt with by Egerton (1860)] under the species that had page priority, namely *Cheiracanthus murchisoni*.

Traquair (1895, plate 2, figure 2) provided an accurate restoration of *Cheiracanthus murchisoni*. The last published reconstruction of *Cheiracanthus murchisoni* was by Watson (1935, figure 22). Later, Watson (1937) described the morphology of *Cheiracanthus murchisoni* in some detail, particularly the head. He noted some morphological differences between *C. murchisoni* and *Cheiracanthus latus*. The scales, however, were hardly mentioned at all. Gross (1947) was the first to give detailed descriptions and illustrations of the crown morphology and the histology of the scales, and Ørvig (1951) was the first to investigate the histological structure of the endoskeleton of *Cheiracanthus murchisoni*, using specimens from Gamrie. He found no traces of perichondral bone, only globular calcified cartilage. He also noted that the rings of Liesegang in the cartilage globules tended to be somewhat polygonal, rather than the circular shape found in the arthrodires.

Miles (1966) briefly compared the Middle Devonian German form *Protogonacanthus* with *Cheiracanthus murchisoni*, and later (Miles, 1973) described and illustrated 'ceratotrichia' in the fins.

Denison (1979, figures 9E, 10J, 31D) reproduced some of Gross' illustrations of scale histology, as well as his own illustration of a scale crown, and detailed the diagnostic features of the species.

Young (1995, figure 9) drew and described the scales of *Cheiracanthus murchisoni* from two regions of the body, above and below the lateral line.

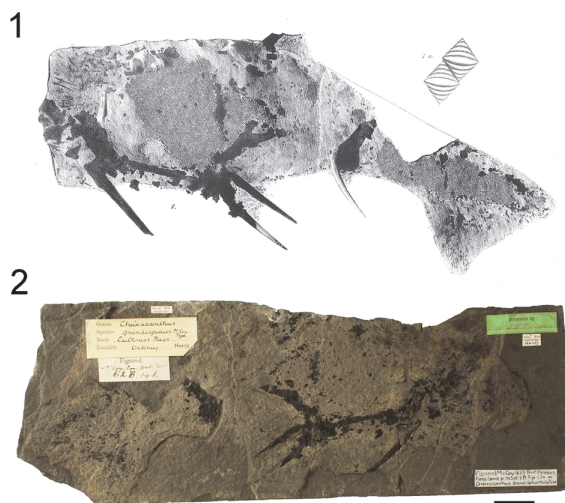


FIGURE 3. *Cheiracanthus grandispinus* holotype SM H4423 from Orkney. 1, mirrored illustration of specimen and scales from M'Coy (1855, plate 2.B, figure 1); 2, specimen in present condition. Scale bar equals 20 mm.



FIGURE 4. *Cheiracanthus latus* Egerton, 1861 holotype from Tynet Burn. 1, NHMUK PV P3253, half of specimen not previously figured; 2, half of the holotype specimen illustrated by Egerton (1861, plate 10, figure 1, 2), now lost. Scale bar equals 20 mm.

One interesting recent paper described the preservation of internal organs of *Cheiracanthus* (Davidson and Trewin, 2005). Two *Cheiracanthus* specimens from Tynet Burn that were figured by Davidson and Trewin (2005, figure 2A, 2B) (NMS G.2000.65.1, 2) are now known to be *Cheiracanthus murchisoni*.

***Cheiracanthus grandispinus* McCoy, 1848**

Cheiracanthus grandispinus was erected by McCoy but not figured at that time. Later, he figured the holotype specimen SM H4423 and gave a fuller description, including detail of the ornamentation of the scale crowns (McCoy, 1855, plate 2.B, figure 1, 1a; Figure 3). (All the figured specimens in his plate are mirror images of the actual specimens.) Both Egerton (1860) and Traquair (1888) concluded that *C. grandispinus* was a valid species. No work of note has since been done on the species.

***Cheiracanthus latus* Egerton, 1861**

Cheiracanthus latus was first erected and figured by Egerton (1861, plate 10, figures 1, 2; Figure 4), with his description based on some 50 specimens from Tynet Burn. He figured only one specimen, but that half of the original nodule is now lost. However, the other half (NHMUK PV P3253) has been located and is now defined as the holotype. Egerton (1861) distinguished the species from *Cheiracanthus latus* Egerton, 1861 by the body being relatively short and thick, having a broad tail and large fin webs with the ventral fins closely approximated; he did not recognise the diagnostic character of the ornamentation of the

scale crowns. He also listed small conical teeth as a character, although he stated that these teeth were not preserved in any of the 50 or so specimens he examined.

Traquair (1888) concluded that *Cheiracanthus latus* Egerton, 1861 was a valid species, as did Woodward (1891), who did not identify any type specimens in the NHMUK collection.

Watson (1937) described the morphology of in some detail, particularly the head. He noted some morphological differences between and *Cheiracanthus latus* Egerton, 1861. The scales, however, were hardly mentioned at all. Gross (1947) was the first author to describe the crown morphology and the histology of the scales in detail.

Miles (1966) briefly compared the Middle Devonian German form *Cheiracanthus latus* Egerton, 1861 with *Cheiracanthus latus*, and later (Miles, 1973) described and illustrated the structure of the shoulder girdle.

Denison (1979, figures 30B, 31A-C) reproduced Miles' (1973) illustration of the shoulder girdle structure and also figured a scale crown, as well as reproducing Watson's reconstruction of the fish.

Young (1995, figure 8) described the scales of *Cheiracanthus latus* and figured the scale crown forms above and below the lateral line anterior the pelvic fins, as well as posterior to the dorsal fin.

Newman et al. (2019) described the histology of *Cheiracanthus latus* spines when comparing against the genus *Haplacanthus*. They also discuss the nature of the base of insertion in *Cheiracanthus*.

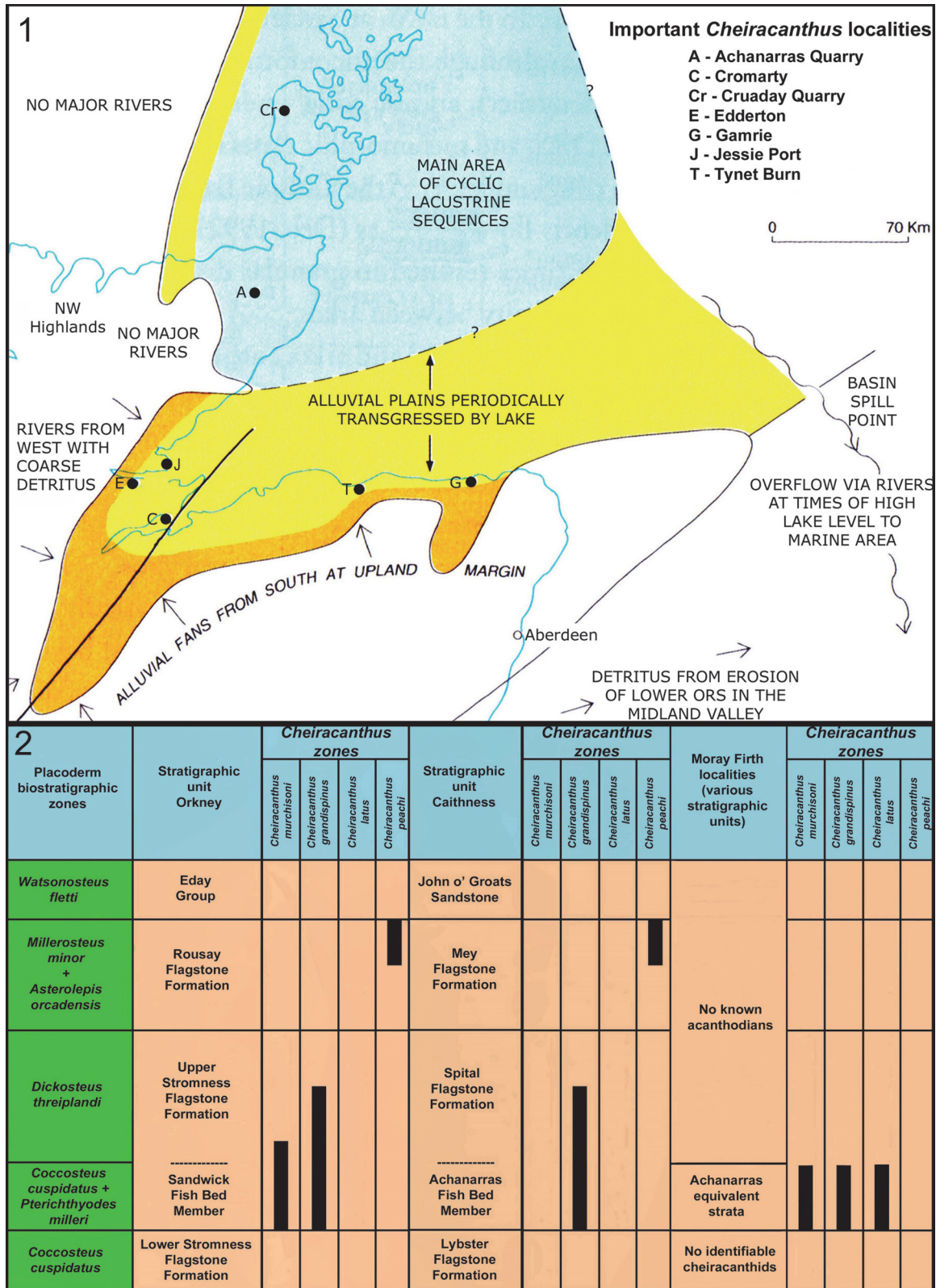


FIGURE 5. 1, Site map indicating the most important localities in northern Scotland where Middle Devonian *Cheiracanthus* specimens have been collected, land in white, current shoreline in blue, alluvial plains in yellow, alluvial fans in ochre; main lake area in blue; 2, biostratigraphic table of *Cheiracanthus* species occurrences in the Orcaidian Basin of northern Scotland. Modified from Burrow et al. (2016, figure 2).

GEOLOGICAL SETTING

Burrow et al. (2016) discussed the geological setting of the Orcadian Basin in the Middle Devonian. In Figure 5 we show the localities of note in the basin and the distribution of *Cheiracanthus* species in relation to Caithness and Orkney stratigraphic units.

In Orkney, *Cheiracanthus* first appears in the Sandwich Fish Bed Member. This horizon is dominated by the species *Cheiracanthus murchisoni*, with *Cheiracanthus grandispinus* being much rarer. Both species continue into the overlying Upper Stromness Flagstone Formation, with *C. grandispinus* surviving the longest, into the middle of this formation. *Cheiracanthus latus* is unknown in Orkney. Another species, *Cheiracanthus peachi*, is found much higher, in the upper part of the Rousay Flagstone Formation.

In Caithness, *Cheiracanthus grandispinus* appears first and is confined to the Achanarras Fish Bed Member. *Cheiracanthus murchisoni* and *Cheiracanthus latus* are unknown in Caithness. As in Orkney, *Cheiracanthus peachi* is found up high in the stratigraphical sequence, in the upper part of the Mey Flagstone Formation. At least one undescribed *Cheiracanthus* species occurs below the Achanarras Fish Bed Member in the Lybster Flagstone Formation and will be the subject of a future project by the authors.

In the nodule beds of the Moray Firth, stratigraphically equivalent to the Achanarras Fish Bed Member, *Cheiracanthus murchisoni*, *Cheiracanthus grandispinus*, and *Cheiracanthus latus* are present, except for Edderton where *C. latus* is absent. Some of the nodule beds at Cromarty might be a little lower than the Achanarras Fish Bed Member and possibly contain the same *Cheiracanthus* species that is present in the Lybster Flagstone Formation. This is under investigation by the authors. Acanthodians are unknown from higher strata in the Moray Firth area.

MATERIALS AND METHODS

Articulated fish were photographed using a Canon EOS 450D. The scale morphologies from squamation patches on NMS G.2019.3.6 and QMF60004, 60005 were imaged by CJB using a JEOL JSM-6300F scanning electron microscope (SEM) housed in the Centre for Microscopy and Microanalysis, University of Queensland, Brisbane, Australia. Preservation of histological structure of the hard tissues varies according to the locality. Often the localities where the fish are preserved in

nodules show good histology, with a few exceptions like Tynet Burn and Edderton. The scales in sections from Tynet Burn are often very translucent and lack the finer histological details, and those from Edderton are brown but also lack some detail. Although fish at Achanarras are very flattened, the preservation of histology is often very good including the fine tubules and the growth boundaries. Other localities that show the histology well are Gamrie and Cromarty, and often the material from the coast north of Hilton. Histology of the fish from the Sandwich fish bed at Orkney is usually poorly preserved, with sections needing to be made very thin in order to make them translucent enough to study the histology.

Thin sections of specimens were made by JdB of specimens using epoxy resin and various grain sizes of corundum grinding powder down to 4 microns, with sections photographed using a Sony DSC-H2 camera on a Nikon Eclipse E400 microscope. Serial sections were made through the head-branchial regions, pectoral region and pectoral fin spine, mid-body region, and tail region of *Cheiracanthus murchisoni* specimen NMS G.2019.3.6 (Figure 6.1, 6.2) from Gamrie after the two halves of the nodule were glued together with Araldite. The slices numbered 2-34, 36-38 on Figure 6.2, in that order, are thin sections NMS G.2019.3.6.2 to NMS G.2019.3.6.34, NMS G.2019.3.6.36 to NMS G.2019.3.6.38, with NMS G.2019.3.6.22 (from the counterpart) and NMS G.2019.3.6.35 (from the part) being samples taken for scanning electron microscopy of scales; dotted lines indicate which side of the slices are glued to the glass slides. Slices 32 and 33 were only made through the counterpart. Pectoral and pelvic fin spines on *C. grandispinus* specimen NMS G.2019.9.7, from Achanarras, were also sectioned (Figure 6.3, 6.4). A medium-sized *Cheiracanthus latus* specimen NMS G.2019.3.3 from Jessie Port was also sectioned (Figure 6.5, 6.6), through squamation patches, the pectoral region and the head (the latter regions were buried below the surface). The slices numbered 2-20 on Figure 6.6 correspond to thin sections NMS G.2019.3.3.2 to NMS G.2019.3.3.20; 1-17 are vertical sections, and 18, 19 are horizontal sections. A small- to medium-sized *Cheiracanthus latus* specimen NMS G.2019.3.7 from Gamrie was also sectioned (Figure 6.7, 6.8); slices numbered 2-20 correspond to thin sections NMS G.2019.3.7.2 to NMS G.2019.3.7.20.

MHNN specimen images downloaded from: <https://commons.wikimedia.org/wiki/>

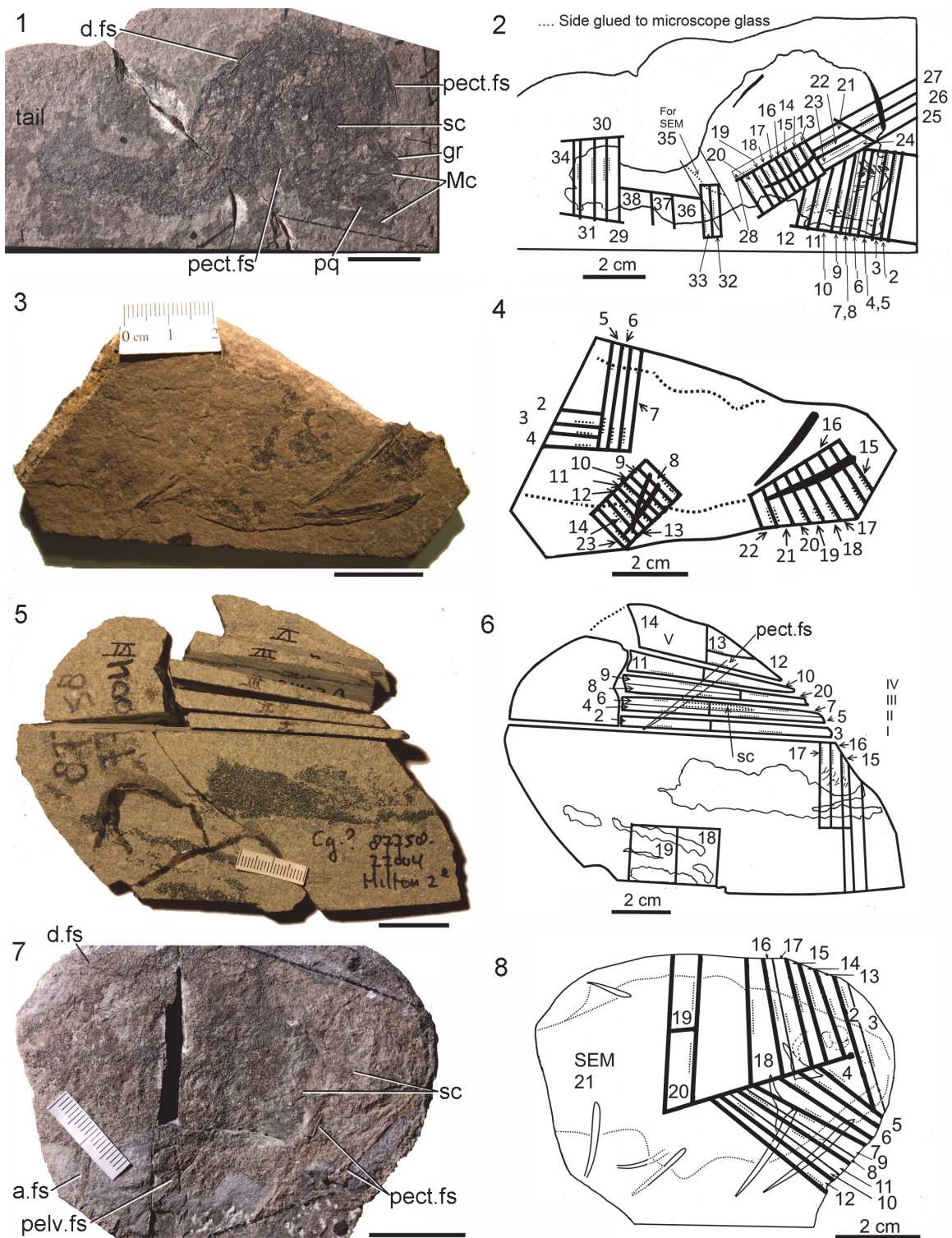


FIGURE 6. Specimens sacrificed for thin sectioning; numbered slices are vertical unless indicated. 1, 2, *Cheiracanthus murchisoni* NMS G.2019.3.6 from Gamrie; slices 36-38 horizontal. 3, 4, *Cheiracanthus grandispinus*, NMS G.2019.9.7 from Achanarras. 5, 6, *Cheiracanthus latus* NMS G.2019.3.3 from Jessie Port; slices 18, 19 horizontal. 7, 8. *Cheiracanthus latus* NMS G.2019.3.7 from Gamrie. Scale bars equal 20 mm. a.fs, anal fin spine; d.fs, dorsal fin spine; gr, gular rays; Mc, Meckel's cartilage; pect.fs, pectoral fin spine; pelv.fs, pelvic fin spines; sc, scapulocoracoid; SEM, area where scales were removed for scanning electron microscopy; small numbers indicate suffix on NMS G specimen number for each thin section.

Category:Media_contributed_by_Mus%C3%A9um_d%27histoire_naturelle_de_Neuch%C3%A2tel;
SM specimen images downloaded from:
<http://www.3d-fossils.ac.uk>.

SYSTEMATIC PALAEOLOGY

Class ACANTHODII Owen, 1846
Order ACANTHODIFORMES Berg, 1940
Family CHEIRACANTHIDAE Berg, 1940

Diagnosis. Acanthodiforms with a short branchial region completely covered by slender branchiostegal rays; jaw cartilages formed of a single mineralisation composed of calcified cartilage blocks; palatoquadrate with median fenestra; mandibular splints absent; 4-6 sclerotic bones; multicuspid denticles/gill rakers on some of the branchial arches; high slender scapular shaft; ossified coracoid and procoracoid; in spines with smooth rounded leading edge ridge separated by groove from smooth or ridged lateral surfaces; dorsal spine with mineralised basal cartilage; no prepelvic or admedian fin spines; polygonal tesserae on cranial roof; ornamented scale crowns.

Remarks. Denison (1979) assigned all acanthodiforms to the one family Acanthodidae, following the suggestion by Miles (1966) that the previous division of the group into the Mesacanthidae, Cheiracanthidae, and Acanthodidae represented a grade, rather than clade, classification. Our observations show that the endoskeletal tissue structure in the Cheiracanthidae (i.e., *Cheiracanthus* and *Homalacanthus*, excluding *Protogonacanthus*), and their ornamented rather than smooth scales, indicate this family is not intermediate between the Mesacanthidae and Acanthodidae and should be considered a legitimate clade.

Genus CHEIRACANTHUS Agassiz, 1835

Type species. *Cheiracanthus murchisoni* Agassiz, 1835

Diagnosis. See den Blaauwen et al., 2019.

Included species. *Cheiracanthus brevicostatus* Gross, 1973, *Cheiracanthus crassus* Valiukevičius, 1985, *Cheiracanthus flabellcostatus* Pinakhina, 2018, *Cheiracanthus gibbosus* Valiukevičius, 1986, *Cheiracanthus grandispinus* McCoy, 1848, *Cheiracanthus intricatus* Valiukevičius, 1985, *Cheiracanthus kaljutensis* Plax, 2018 (in Plax and Zaika, 2018), *Cheiracanthus kruckeki* Valiukevičius, 1986 (in Valiukevičius and Karatajūtė-Talimaa, 1986), *Cheiracanthus latus* Egerton, 1861, *Cheiracanthus peachi* den Blaauwen, Newman and Burrow, 2019, *Cheiracanthus splendens*

Gross, 1973, *Cheiracanthus talimae* Valiukevičius, 1985.

Cheiracanthus murchisoni Agassiz, 1835

Figure 1, Figure 2, Figure 6.1, 6.2, Figures 7-14

- 1835 *Cheiracanthus murchisoni* Agass.; Agassiz, vol. 2 p. 126-127, pl. 1c, figs. 3-4.
1835 *Cheiracanthus minor* Agass.; Agassiz, 127-128, pl. 1c, fig. 5.
1841 *Cheiracanthus*; Miller, p. 86, 88-93, pl. 7, figs. 1-2.
1844 *Cheiracanthus microlepidotus* Agass.; Agassiz, 38-39, pl. 15, figs. 1-3.
1847 *Cheiracanthus microlepidotus* Ag.; Miller, p. 119, 122-126, pl. 7, figs. 1-2.
1848 *Chiracanthus pulverulentus* (M'Coy); M'Coy, p. 299.
1848 *C. murchisoni* (Ag.); M'Coy, p. 299.
1848 *Chiracanthus lateralis* (M'Coy); M'Coy, p. 300.
1855 *Chiracanthus lateralis* (M'Coy); M'Coy, p. 582.
1855 *Chiracanthus microlepidotus* (M'Coy); M'Coy, p. 583.
1855 *Chiracanthus minor* (M'Coy); M'Coy, p. 583.
1855 *Chiracanthus murchisoni* (Ag.); M'Coy, p. 583.
1855 *Chiracanthus pulverulentus* (M'Coy); M'Coy, p. 583, pl. 2B, fig. 2.
1860 *Cheiracanthus lateralis*; Egerton, p. 123.
1860 *Cheiracanthus minor*; Egerton, p. 123.
1860 *Cheiracanthus pulverulentus*; Egerton, p. 123.
1861 *Cheiracanthus murchisoni*; Egerton, p. 73.
1861 *Cheiracanthus microlepidotus*; Egerton, p. 73-74.
1861 *Cheiracanthus minor*; Egerton, p. 73.
1861 *Cheiracanthus pulverulentus*; Egerton, p. 73.
1888 *Ch. murchisoni*, Ag.; Traquair, p. 512.
1890 *Cheiracanthus murchisoni*; Woodward and Sherborn, p. 29-30.
1891 *Cheiracanthus murchisoni*, Agassiz; Woodward, p. 16-18.
1907 *Cheiracanthus murchisoni*; Dean, p. 213.
1927 *Cheiracanthus murchisoni* Ag. 1835 (t.), 1836 (p.); Jeannet, p. 106.
1927 *Cheiracanthus microlepidotus* Ag. 1844; Jeannet, p. 106.
1935 *Cheiracanthus murchisoni* Agassiz; Watson, p. 158, fig. 22.
1937 *Cheiracanthus murchisoni* Ag.; Watson, p. 84-88, fig. 12, pl. 12, figs. 1-3.
1940 *Cheiracanthus murchisoni* Agassiz; Berg, p. 129, fig. 21B.
1947 *Cheiracanthus murchisoni* AG; Gross, p. 124-125, fig. 13A-F, pl. 25, fig. 5.
1951 *Cheiracanthus murchisoni*; Ørvig, p. 414.

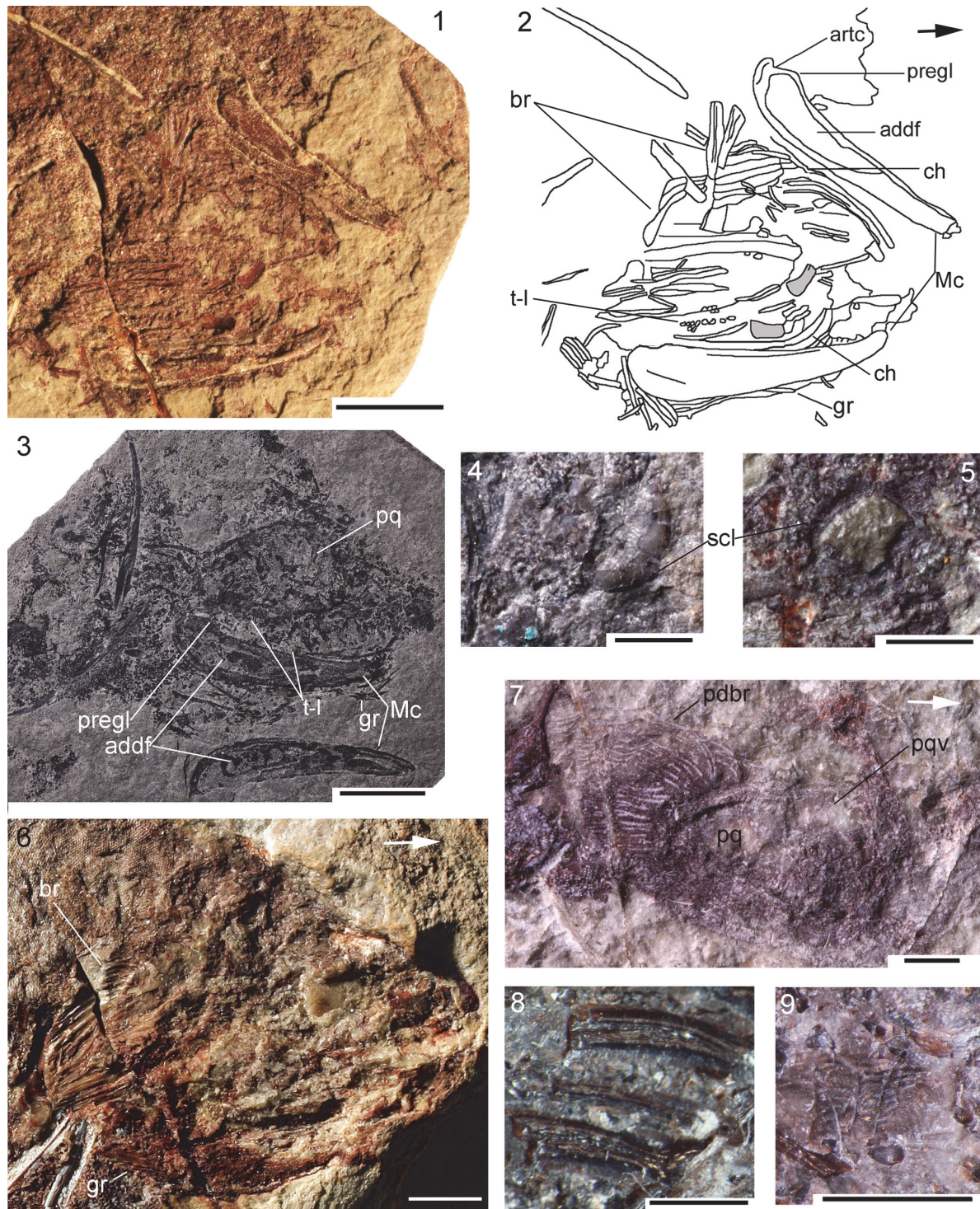


FIGURE 7. *Cheiracanthus purchisoni* head and branchial region morphology. 1, 2, NMS G.1884.60.3 from Tynet Burn. 3, NMS G.2019.9.24 from Cruaday Quarry, Orkney. 4, NRM P1651 from Gamrie, sclerotic ring. 5, NRM P1654 from Tynet Burn, sclerotic ring. 6, NMS G.2000.65.2 from Tynet Burn. 7, NMS G.2019.14.2 from Tynet Burn. 8, 9, NRM P1560 from Gamrie: 8, detail of branchiostegal rays; 9, impression of spiracular valve. Scale bars equal 10 mm in 1, 3, 6, 7; 5 mm in 4, 5; 2 mm in 8, 9. addf adductor muscle fossa; artc, articular cotylus; br, branchiostegal rays; ch, ceratohyal; gr, gular rays; Mc, Meckel's cartilage; pabr, posterodorsal branchiostegal rays; pq, palatoquadrate; pqv, palatoquadrate vacuity; pregl, preglenoid process; scl, sclerotic plate; t-l, tooth-like elements. Arrows indicate anterior.

- 1966 *Cheiracanthus murchisoni* Ag.; Miles, p. 159, 161, fig. 8F.
- 1970 *Cheiracanthus murchisoni* Agassiz; Miles, p. 362.
- 1973 *C. murchisoni* Agassiz; Miles, p. 157, pl. 20.2
- 1976 *Cheiracanthus murchisoni* Agassiz 1835; Paton, p. 18.
- 1976 *Cheiracanthus murchisoni*; Zidek, p. 23.
- 1979 *Cheiracanthus murchisoni*; Denison, figs. 9E, 10J, 31D.
- 1979 *C. murchisoni* Agassiz 1835; Denison, p. 47.
- 1995 *Cheiracanthus murchisoni*; Young, p. 68, fig. 9.
- 1996 *Cheiracanthus murchisoni*; Gagnier, p. 162.
- 1997 *C. murchisoni*; Young, p. 48.
- 1999 *Cheiracanthus murchisoni*; Dineley and Metcalf, ch. 6, Den of Findon p. 1, 3; Cruaday Quarry fig. 6.12E, F; Tynet Burn fig. 6.20B.
- 1999 *Cheiracanthus murchisoni* Agassiz, 1835; Dineley and Metcalf, ch. 6, Den of Findon p. 3; Achanarras Quarry p. 3; Cruaday Quarry p. 3; Black Park p. 3.
- 1999 *C. murchisoni* Agassiz, 1835; Dineley and Metcalf, ch. 6, Tynet Burn p. 3.
- 2005 *Cheiracanthus*; Davidson and Trewin, p. 131, table 1, fig. 2A, 2B.
- 2005 *Cheiracanthus murchisoni*; Newman and Dean, p. 4.
- 2005 *C. murchisoni*; Newman and Dean, p. 4.
- 2005 *Cheiracanthus murchisoni* Agassiz, 1835; Burrow and Young, p. 13.
- 2010 *Cheiracanthus murchisoni*; Sallan and Coates, p. 24.
- 2015 *Cheiracanthus murchisoni*; Taylor and O'Dea, p. 51, 216, fig. on pp. 50-51.
- 2018 *Cheiracanthus murchisoni* Agassiz, 1835; Glinskiy and Pinakhina, p. 83.
- 2019 *Cheiracanthus murchisoni* Agassiz, 1835; Newman, Burrow and den Blaauwen, p. 5.

Holotype. MHNN FOS 39 from Lethen Bar.

Material examined. From Lethen Bar: MHNN FOS 40, 41; NHMUK PV P544; NMS G.1891.92.323; NMS G.1966.40.23; NMS G. 1972.23.1; NMS G.1973.12.106; NMS G.1973.12.109; NMS G.1973.12.120; NMS G.1973.12.116; NMS G.1973.12.130; NMV P30172. From Tynet Burn: NMS G.1877.30.2; NMS G.1884.60.3; NMS G.2000.65.1; NMS G.2000.65.2; NMS G.2019.14.1; NMS G.2019.14.2; NRM P1638; NRM P1654; QMF60005. From Gamrie: NMS G.1891.92.8.1; NMS G.1891.92.306; NMS G.1891.92.307; NMS G.1975.12.8; NMS G.2019.3.6; NMV P29277; NMV P29286; NMV P29287; NRM P1650. From Geanies Point, Tarbat Ness Peninsula: NMS G.2019.14.3. From Cromarty: NMS G.1953.4.2;

NMS G.2019.9.25; NMS G.2019.9.29; NMS G.2019.9.32. From Jessie Port, Tarbat Ness Peninsula: NMS G.2019.14.6; NMS G.2019.9.33. From Edderton, Ross and Cromarty: NRM P4260; NMS G.2019.9.27; NMS G.2019.9.28; NMS G.2019.9.30. From Tarbat Ness: NMS G.2019.9.26 (this is from below the Achanarras horizon). From Den of Findon: NMS G.2019.9.31. From the Moray Firth area: NMS G.1870.14.171; NMS G.1882.16.13; NMS G.1981.39.36. From Cruaday Quarry: NMS G.2019.9.24. From Hooveth, Orkney: NMS G.1899.83.5; From Instabillie, Orkney: NMS G.1898.163.4. From Orkney: SM H 4424; SM H 4425.

Distribution. Nodule beds stratigraphically equivalent to the Achanarras Fish Bed Member, Moray Firth; Sandwick Fish Bed Member and Upper Stromness Flagstone Formation (Eifelian), Orkney; ?undetermined levels in the Narva Regional Stage (R.S.), Baltic countries.

Diagnosis. *Cheiracanthus* with more than 20 contiguous long, robust, branchiostegal rays with straight posterior ends; several fine thin rays above the main branchial cover; fine thin gular rays below the jaws; slender, dorsally-tapering scapular shaft, height 10 times its minimum width; spiracle with pair of comma shaped valves; pectoral spine with low sharp-crested ridges along lateral faces; scale crowns ornamented with non-branching subparallel ridges extending from the anterior edge and terminating before mid-crown; some scales with a posterior median pit on the crown; scale crown growth zones with straight posterolateral edges.

Description. General features: The dorsal fin spine is positioned halfway between the pelvic and anal spines. On all fish, the pelvic spines are always the shortest, about 60 percent of the length of the dorsal spine. The anal spine is intermediate in length between that of the dorsal and pelvics, about 70 to 75 percent the length of the dorsal spine. The pectoral spine is variable in length, and can be shorter than, equal in length, or longer than the dorsal spine.

Head and branchial region: Watson (1937, figure 12) detailed the main morphological features of these regions, so we only present an overview and describe new observations (Figure 7). The lower jaw Meckel's cartilages are always mineralised as a single unit as are the palatoquadrates, but these are less frequently mineralised, and are also often not preserved intact but as scattered patches. We note that the fossa for insertion of the adductor muscle on the lateral side of the Meckel's cartilage (Figure 7.1-3) extends about half the length of the

jaw. The ventral margin of the cartilage is thickened to form a ridge along this edge. The small preglenoid process is quite rounded, and the articular cotylus is a shallow embayment, slightly longer than wide. Tooth-like structures are present in the mouth (Figure 7.1-3). These are possibly equivalent to similar elements in *Homalacanthus concinnus*, where they are distributed in rows near the upper edge of the Meckel's cartilage and the lower edge of the palatoquadrate (Schultze, 1972, figure 2).

The two main dermal elements of the head and branchial region are the orbital bones and the branchiostegal rays. The former comprise 4-6 sclerotic plates (Figure 7.4, 7.5), not circumorbital bones as described by Watson (1937); see Burrow et al. (2011). Disarticulated sclerotic plates (Figure 7.1, 7.2: shaded grey) show that they are short, curved, and mesially concave. In articulation they are close-set (Figure 7.4). The internal surface is smooth, but the external surface on at least some specimens was ornamented with fine, sinuously radiating ridges (Figure 7.5). The ornament layer appears very thin and is rarely preserved intact (Figure 7.4).

The dermal branchiostegal rays are as Watson (1937) described them (Figure 7.6, 7.7), with c. eight below the angle of the jaw and 16 or more above the jaw angle; some of the larger rays have an ornamentation of two ridges running parallel to their long edges (Figure 7.8). As noted by Watson (1937), the most dorsal branchiostegal rays of the main cover are fairly flat with no abrupt bends to the ventral on the posterior ends of the individual rays (Figure 7.6). We observe that there are also long thin rays above the main branchial cover (Figure 7.7). These are much more fragile than the branchiostegal rays and are rarely preserved. Short delicate rays are present between the dorsal area of main branchial cover and the shoulder girdle (Figure 7.7). Watson (1937, p. 87, figure 12; plate 12, figure 3) described "two small sickle-shaped bones" above the main branchial cover on NHMUK PVP.43273 that he identified as the upper end of the hyoid arch. Based on their position and circular arrangement, we interpret these elements as the dermal spiracular valve (Burrow et al., 2020). The internal pseudobranch is also seen as an impression on NRM P1650 (Figure 7.9) and in thin section on NMS G.2019.3.6.15 (see next section). Thin gular rays are also present below the jaws (Figure 7.7). Elements not previously identified are denticles in the branchial region, presumed to have been borne on the branchial arches (Figure 7.1, 7.2; see next section).

Thin sections (Figure 8) show that the jaws and at least some other endoskeletal structures in these regions are preserved as a layer of calcified cartilage (cc), often formed of contiguous blocks which are sub-rectangular in vertical section (Figure 8.1). In other areas, the cartilage layer is formed of separated irregularly shaped blocks (Figure 8.2-6). Rings and lines of Liesegang are sometimes visible within the cc blocks (Figure 8.2). The jaw cartilages are preserved as a single-layer of cc blocks enclosing a calcitic core, presumed to have originally been unmineralised cartilage. Both dorsal and ventral edges of the jaws are thickened, but still encased with just a single layer of cc blocks (Figure 8.6).

Flat or slightly concave based dermal tesseræ are borne directly on the cartilage blocks (Figure 8.3, 8.5). The sensory lines on the head are enclosed by paired specialised scales with thin flat bases and thin crowns that arch over and meet along the median line between the two rows of scales (Figure 8.7, 8.9). The scale crowns are formed of superposed growth zones. Tesseræ above the jaws have a thick base penetrated by Sharpey's fibres and a dentinous crown showing apposed growth zones (Figure 8.8).

The anteriormost branchial arches are formed of a two-layered, consolidated cc, with the outer layer appearing denser than the inner layer (Figure 8.10, 8.11). This two-layered structure perhaps equates with a mesodermal and neural crest derived origin for the outer and inner layers respectively, based on comparison with the development of the gill arches in skate embryos (see Gillis and Tidswell, 2017, figure 2c).

Some of the branchial arches (e.g., Figure 8.10) are surrounded by small plates with a long inclined pointed crown, which we identify as branchial denticles. Other larger elements in the branchial region show a vertical section similar to that of the branchial denticles, but have a large pulp cavity and a dentine crown (Figure 8.12, 8.13). We identify these elements as equivalent to the supposed gill rakers of the cheiracanthid *Homalacanthus concinnus*. Schultze (1972, figure 4) described these as teeth, but Zidek (1985) subsequently suggested that they were gill rakers, agreeing with Schultze that the outer layer was dentine and so, like teeth, they were dermal structures. We are unable to determine the exact distribution of the elements in *C. purchisoni*, but refer to them as tooth-like elements as it seems likely that, as in *H. concinnus*, they are only found near the edges of the palatoquadrate and Meckel's cartilage rather



FIGURE 8. *Cheiracanthus purchisoni* head and branchial region histology. Thin sections of NMS G.2019.3.6 (see Figure 6.2 and text for position of sections). 1, NMS G.2019.3.6.2, Meckel's cartilage; 2, NMS G.2019.3.6.7, calcified cartilage block showing rings of Liesegang; 3, NMS G.2019.3.6.3, separated calcified cartilage blocks overlain by dermal tessera; 4, NMS G.2019.3.6.4, cc and ?subcylindrical sensory line scale; 5, cc of palatoquadrate with dermal tesserae and pair of scales in vertical longitudinal section, edging sensory line; 6, NMS G.2019.3.6.6, ridge on dorsal edge of palatoquadrate cartilage, calcite infilling; 7, NMS G.2019.3.6.9, pair of sensory line scales, oblique section through base and lower crown; 8, NMS G.2019.3.6.12, dermal tesserae, vertical transverse sections; 9, NMS G.2019.3.6.9, pair of sensory line scales, vertical transverse section; 10, NMS G.2019.3.6.7, ceratohyal and another branchial arch; 11, NMS G.2019.3.6.6, branchial arches; 12, 13, NMS G.2019.3.6.9, ?tesserae and ?denticle of the branchial region; 14, 15, NMS G.2019.3.6.5, branchiostegal plates and calcified cartilage, with closeup of branchiostegal transverse section; 15, tessera with polyodontode crown on globular calcified cartilage; 16, NMS G.2019.3.6.4, branchiostegal plates and gular rays; 17, NMS G.2019.3.6.15, spiracular valve. Scale bars equal 1.0 mm. ba, branchial arches; br, branchiostegal plate/ray; cc, calcified cartilage; ch, ceratohyal; d, denticle; gr, gular rays; t, tessera; ?, indeterminate element, possibly subcylindrical sensory line scale.

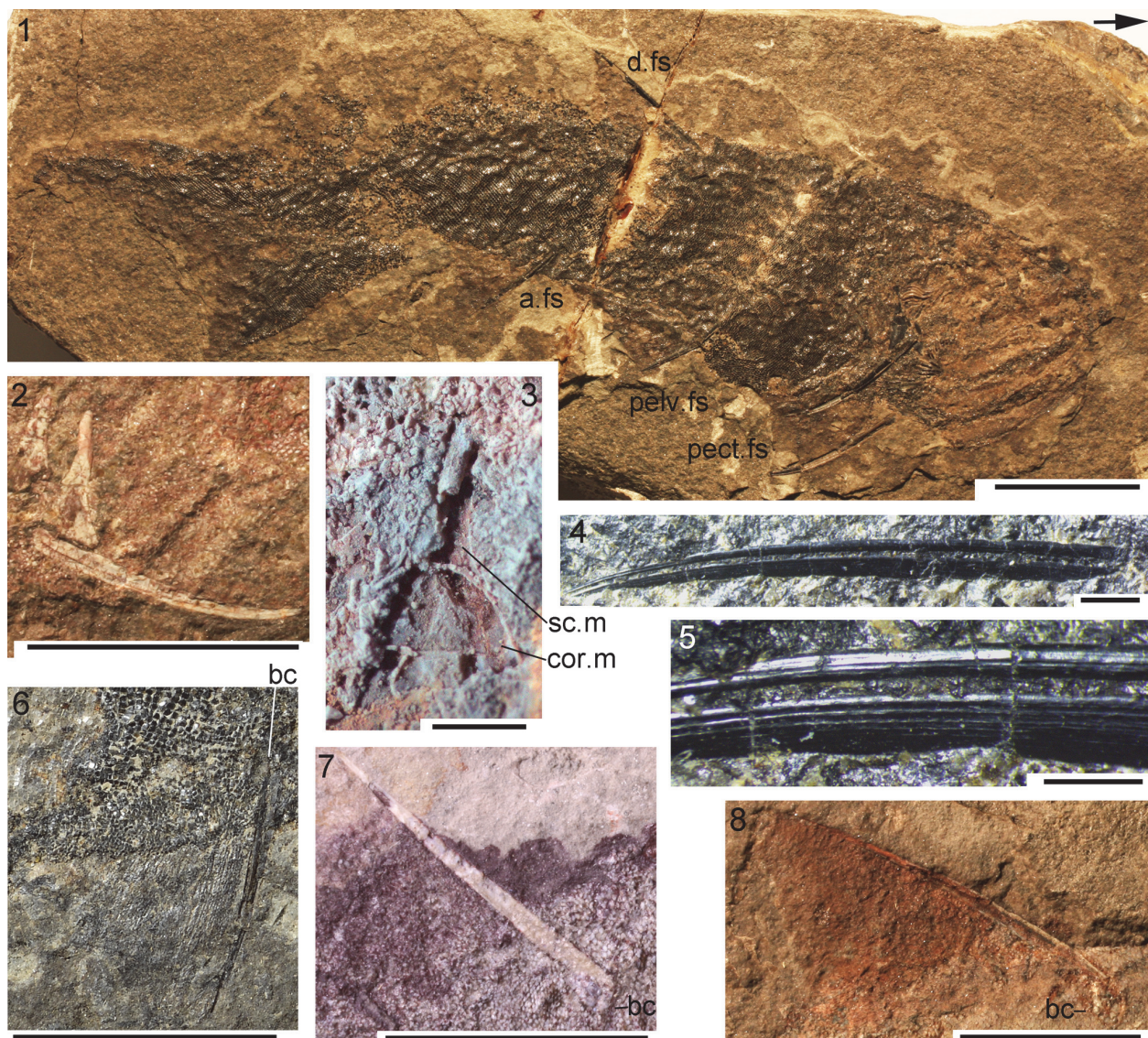


FIGURE 9. *Cheiracanthus murchisoni* spines and scapulocoracoid morphology. 1, NMS G.1891.92.307 from Gamrie, specimen showing disposition and relative sizes of fin spines and scapulocoracoid. 2, NMS G.1973.12.120 from Lethen Bar, articulated scapulocoracoid and pectoral fin spine. 3, QMF60005 from Tynet Burn, scapulocoracoid 'shell' with calcified cartilage core and calcified separation between molds of scapula and coracoid elements. 4, 5, NMS G.2019.9.27 from Edderton, pectoral spine. 6, NMV P29287 from Gamrie, anal fin spine, web, and basal cartilage. 7, NRM P1654 from Tynet Burn, dorsal fin spine with basal cartilage. 8, NMS G.1972.23.1 from Lethen Bar, dorsal fin spine with basal cartilage. Scale bars equal 20 mm in 1, 2, 6-8, 2 mm in 3-5. a.fs, anal fin spine; bc, basal cartilage; cor.m, coracoid mold; d.fs, dorsal fin spine; pect.fs, pectoral fin spine; pelv.fs, pelvic fin spines; sc.m, scapula mold. Arrow indicates anterior.

than being associated with the branchial arches. The dermal branchiostegal plates and smaller gular rays are formed of a dense bone; the ornament layer on the branchiostegal plates is formed of superposed dentine layers (Figure 8.14-16). As noted in the previous section, we have also identified spiracular valves, shown in vertical cross section in Figure 8.17, formed of dense mineralised tissues (Burrow et al., 2020).

Pectoral region and fin spines: The scapulocoracoid has a slender tapering scapular shaft (Figure 9.1-3) with a circular cross section (Figure 10.1). Minimum diameter of the shaft increases very slightly between the smallest and largest fish, being 0.9 mm in the 100 mm long NMS G.1965.59.34 and 2.0 mm in the 205 mm long NMS G.1972.23.1. The height of the scapulocoracoid, however, increases more dramatically, being

6.0 mm in the smallest and 19.0 mm in the largest fish (Table 1). Contra Watson (1937), the ventral edge of the scapulocoracoid is contiguous with the upper surface of the pectoral fin spine, as described by Miles (1973). The line of fusion between the scapula and coracoid is convex upwards (Figure 9.3). Miles (1973) noted that the element sometimes mineralised in front of the fin spine, that Watson (1937) referred to as the coracoid, is in fact the procoracoid.

All the fin spines have only one groove on each side, separating the leading edge ridge from the 'shoulder' (i.e., rounded upper corner) of the sides (Figure 9.1, 9.2, 9.4-6). Towards the base of the spine, the groove becomes deep and narrow. The pectoral fin spine has low, sharp-crested lateral ridges (Figure 9.4, 9.5), which are sometimes also present on the dorsal fin spines. In all spines the inserted part is short, contra Watson (1937, p. 84). The pulp or central cavity of the spines is open posteriorly/along the trailing edge for a considerable distance, up to half the total length on the dorsal spine.

The dorsal fin spine (Figure 9.1, 9.7, 9.8) is almost straight, laterally compressed, with a broadly rounded leading edge ridge; the sides of the ridge are in line with the shoulders and the flanks. The height of the spine increases relative to the width from proximal to distal. The anal fin spine (Figure 9.6) is slightly recurved and also has a broadly rounded anterior rib; the sides are more rounded than on the dorsal spine. Both dorsal and anal spines sometimes have a mineralised basal cartilage preserved (Figure 9.6-8); its presence or absence appears independent of locality.

On the paired pelvic fin spines, the anterior ridge has a more or less triangular shape, and the height to width ratio increases from proximal to distal. The spines are notably asymmetric.

The pectoral spine (Figure 9.1, 9.2, 9.4) is strongly curved lengthwise, relative to the other spines. Like the pelvic spines, the spines are slightly asymmetric in cross section, and the anterior ridge has a sharply pointed triangular shape in cross section. The sides are straight, in line with the sides of the anterior ridge. The height:width ratio increases dramatically from proximal to distal, and the spines are more robust than the other spines.

All spines (exemplified here by the pectoral fin spine, Figure 10.2-7), like those of all *Cheiracanthus* species, have a thin enameloid outer layer on the leading edge and 'shoulders' of the spine, preserved best towards the proximal end, as are the

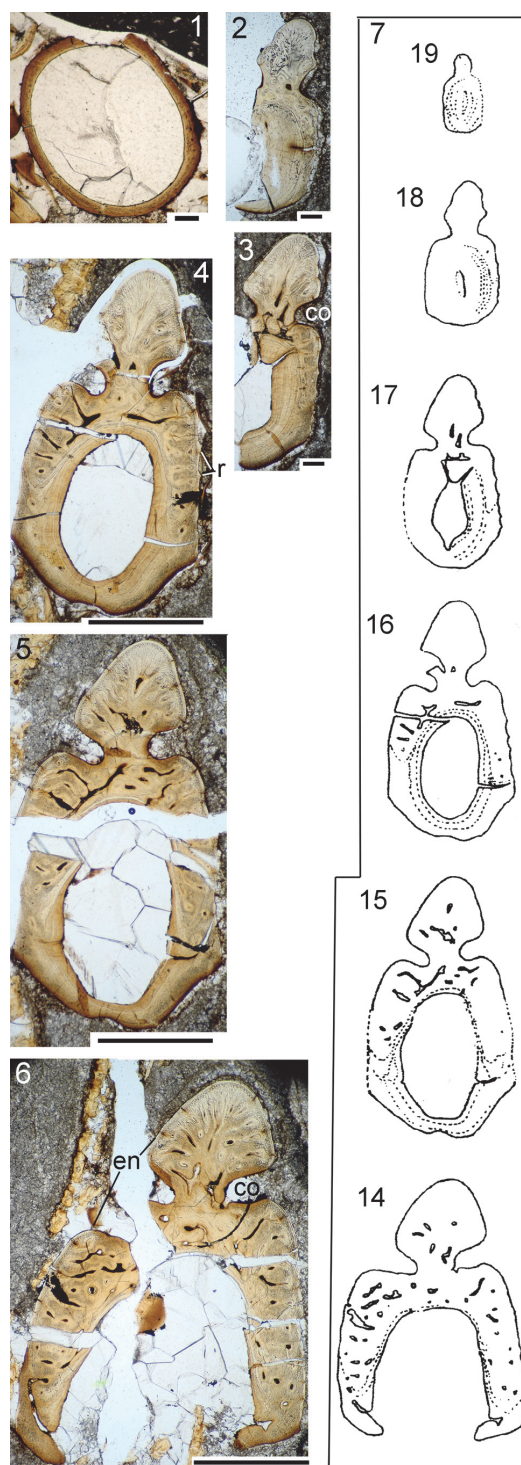


FIGURE 10. *Cheiracanthus purchisoni* NMS G.2019.3.6 from Gamrie, scapula shaft and pectoral spine histology. 1, NMS G.2019.3.6.27, transverse section of scapula shaft. 2-6, transmission microscope images of NMS G.2019.3.6.14, 15, 16, 18, 19; 7, drawings of main histological features in thin sections 19-14, from tip to near the base of the exerted part. Scale bars equal 0.1 mm in 1-3, 0.5 mm in 4-6. co, canal opening; en, enameloid; r, sharp crested lateral ridges.

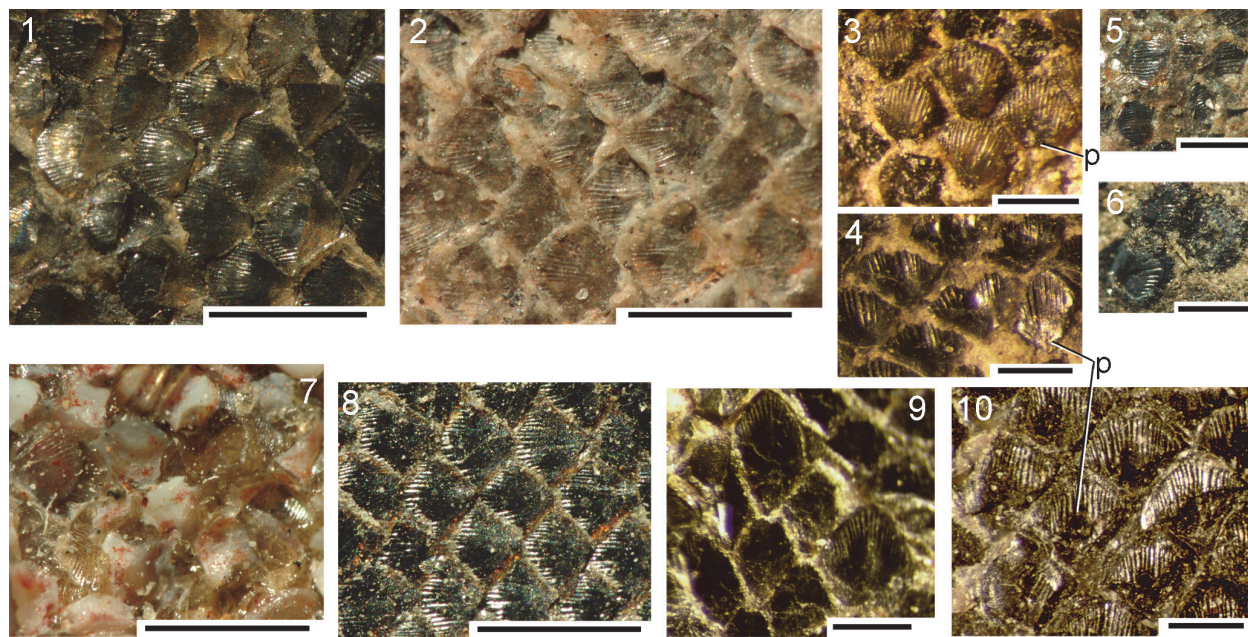


FIGURE 11. *Cheiracanthus murchisoni* squamation: light microscope images, all mid-body scales except 9. 1, NMS G.1892.8.1 from Gamrie. 2, NMS G.1891.92.323 from Lethen Bar. 3, NMS G.2019.9.25 from Cromarty, Suturs. 4, NMS G.2019.9.26 from Tarbat. 5, NMS G.1882.16.13 from Cromarty. 6, NMS G.1899.83.5 from Hooveth, Orkney. 7, NMS G.1877.30.2 from Tynet Burn. 8, NMS G.1968.5.3 from Edderton. 9, NMS G.2019.9.27 from Blackpark, tail. 10, NMS G.2019.9.28 from Blackpark, scales with crown pits. Scale bars equal 1.0 mm in 1, 2, 7, 8; 0.5 mm in 3-6, 9, 10. p, pit on posterior scale crown.

thin sharp-crested lateral ridges. Spines have a wide central cavity, and all spines lack an accessory pulp canal above the central cavity. Osteodentine forms most of the width of the spine proximally. In the leading edge ridge, dentine tubules run perpendicular from the outer surface towards vascular canals running longitudinally. These canals are arranged in concentric, interconnected series, more or less parallel to the outer surface of the spines. Longitudinal and interconnecting canals extend the length and breadth of the whole spine, with smaller canals leading off to open out in the sulcus between the leading edge ridge and the 'shoulders' of the spines, as well as into the central cavity. Denteons are formed around the canals in the exerted part, but not in the inserted part; they increase in thickness distally, with the canals subsequently becoming narrower or almost closed. An inner lamellar layer is present proximal to the closure of the central cavity, and increases in thickness distally. A very thin, dense layer lines the central cavity proximally, and separates the osteodentine layer from the inner lamellar layer through the whole spine. Short dentine tubules extend through each of the lamellar layers, perpendicular to the inner surface. Towards the tip of the

spine, the central cavity is almost filled by the centripetal growth of the inner layers of dentine.

Body scales: Watson (1937) and Gross (1947) described the scales as being relatively uniform over the body, but we note some variation. In the anterior half of the body the width of the scales sometimes slightly exceeds the length, whereas posterior to the anal fin spine the length of the scales often considerably exceeds the width, with the maximum length to width ratio about 2:1. On most flank scales, the crown ornament comprises fine subparallel ridges extending back from the anterior margin (Figures 11.1-8, 11.10, 12.1-6, 12.12-20), which often has a smooth rim on scales of larger fish. The ridges have a rounded surface, do not branch, and terminate in the anterior half of the crown. The length of the ridges varies depending on the area of the body (Figure 11.7-10), with scales above the lateral line tending to have longer ribs than those below (Young, 1995, figure 9). Ridge length also depends on the age of the fish, with larger/older fish having relatively longer ridges than smaller/juvenile fish. Many scales have a median depression longitudinally on the crown surface (Figures 11.3, 11.4, 11.10, 12.5, 12.6, 12.13, and 12.15).

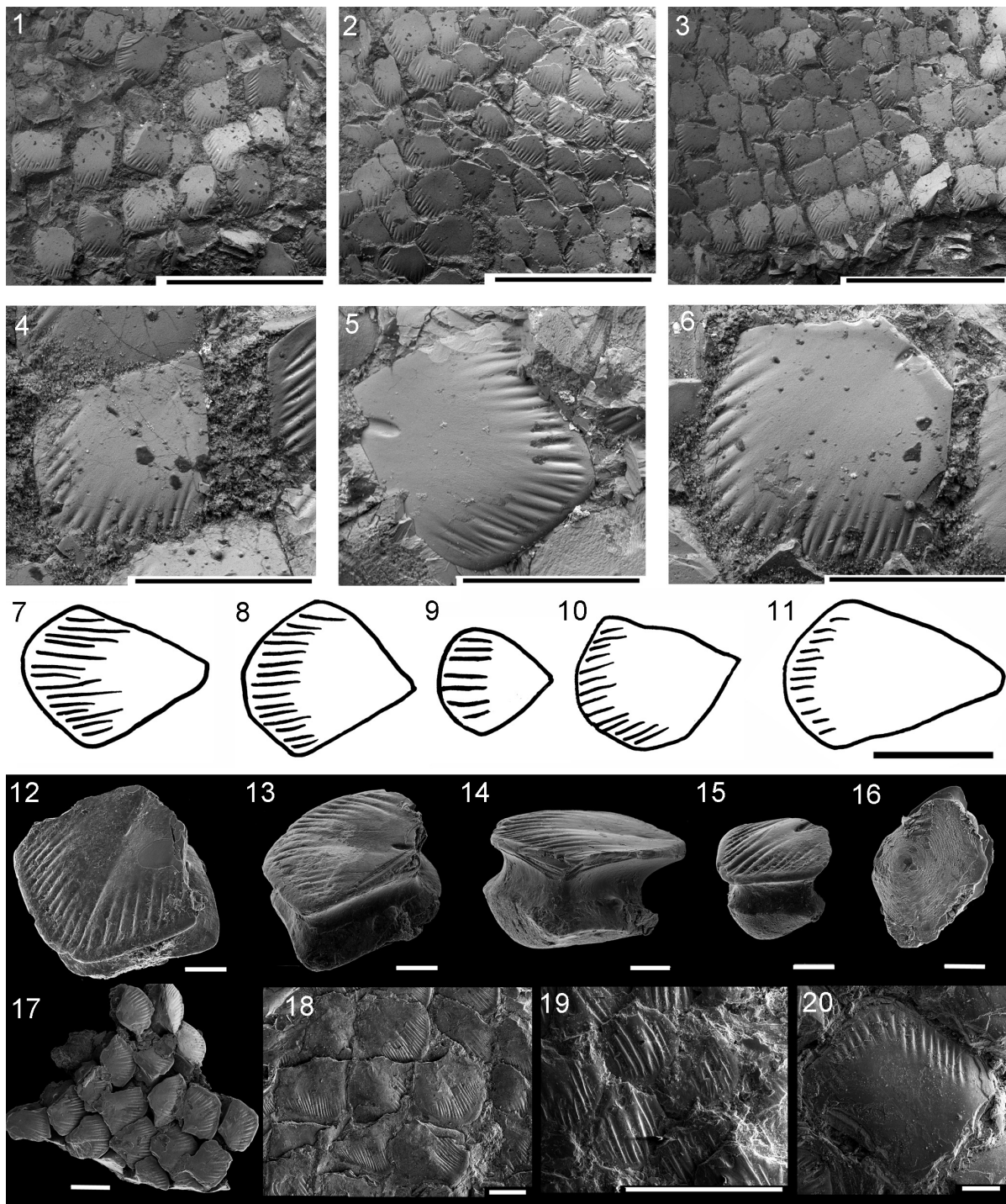


FIGURE 12. *Cheiracanthus murchisoni* scale morphology. 1-11, NMS G.2019.3.6 from Gamrie: 1-6, SEM images of scale patch NMS G.2019.3.6.35 removed from midflank of counterpart; 7-11, drawings of scale crowns from: 7, behind the head; 8, midbody; 9, near the dorsal fin spine; 10, in front of the tail; 11, on the tail. 12-15, SEM images of detached midbody? scales of NMS G.2019.9.29 from Cromarty Sutors: 12, NMS G.2019.9.29.11.5, crown view; 13, NMS G.2019.9.29.11.2, laterocrown view; 14, NMS G.2019.9.29.11.19, lateral view; 15, NMS G.2019.9.29.11.1, anterolateral view. 16, 17, NMS G.2019.9.29.12 from Cromarty Sutors: 16, NMS G.2019.9.29.12.3, base showing concentric lines of Sharpey's fibre bundles; 17, NMS G.2019.9.29.12.2, patch of articulated scales, crown view. 18, 19, ventral mid-body squamation patches of NMS G.2019.9.31.2 from Den of Findon. 20, NMS G.2019.9.30.2 from Edderton, scale in squamation patch. Scale bars equal 1.0 mm in 1-3, 0.3 mm in 4-11 (7-11 all at same scale), 17, 18, 20; 0.1 mm in 12-16, 20.

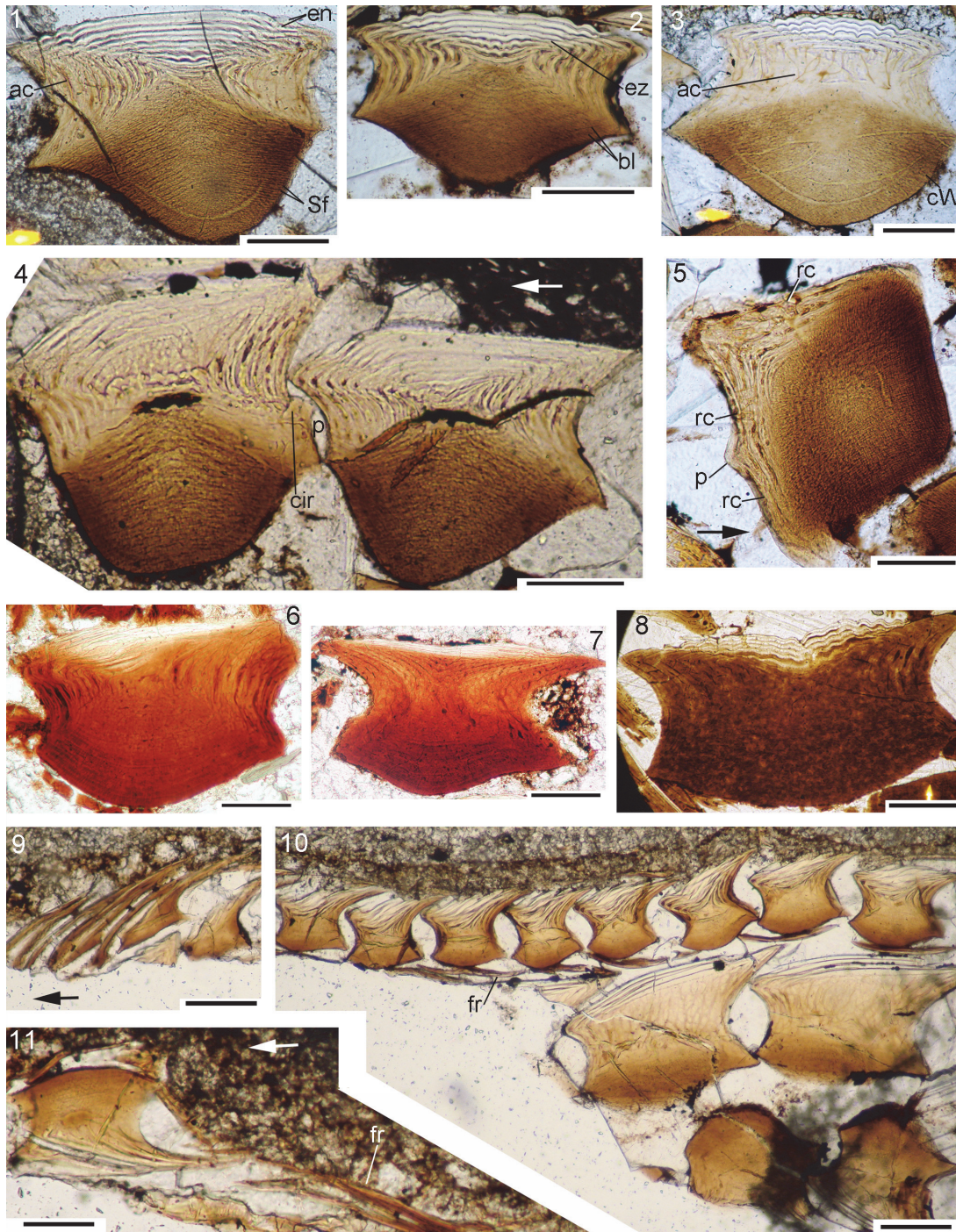


FIGURE 13. *Cheiracanthus murchisoni* scale histology. 1-5, 9-11: thin sections of scales from NMS G.2019.3.6 from Gamrie: 1, NMS G.2019.3.6.20, slightly oblique vertical section of mid-body scale; 2, NMS G.2019.3.6.32, vertical transverse section of ventral scale in the shoulder girdle region; 3, NMS G.2019.3.6.19, vertical transverse section of scale behind the head; 4, NMS G.2019.3.6.33, vertical longitudinal section of two contiguous scales in the midbody flank region; 5, NMS G.2019.3.6.36, subhorizontal section through base and lower crown; 9-11, NMS G.2019.3.6.28, vertical longitudinal section through fin web and body scales near pectoral fin spine: 9, distal fin scales; 10, fin web and body scales; 11, fin web scale and fin rays=ceratotrichia. 6, NMS G.2019.9.29.5 from Cromarty, vertical oblique section. 7, NMS G.2019.9.29.10 from Cromarty Sutors, vertical transverse section through posterior crown; 8, NMS G.2019.9.33.6, from Jessie Port, vertical transverse section. Scale bars equal 0.1 mm. ac, ascending canals; bl, base lamellae; cir, circular canals; cW, canals of Williamson; en, enameloid; ez, embryonic zone; fr, fin ray; lac, canal lacunae; p, protuberance; rc, radial canal; Sf, Sharpey's fibre bundles. Arrows indicate anterior.

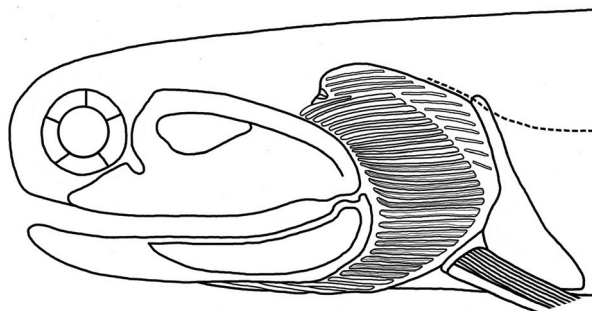


FIGURE 14. *Cheiracanthus murchisoni* head and branchial region reconstruction.

Rows of scales near the lateral lines and also some in other areas have a median pit in the posterior half of the crown (Gross, 1947). Some of these pitted scales have a crown that is otherwise identical to the majority of scales, whereas others have a relatively narrow crown with thicker subparallel ribs extending to the posterior of the crown, around a relatively large pit (Figure 12.19). Scales on the front edge of the tail are larger than body scales and have a totally smooth crown (Gross, 1947). The neck is concave and smooth all round, with a pair of protuberances posteriorly, just above the base-neck rim (Figure 12.13, 12.14). The neck height is almost equal to the height of the base, which is well rounded and penetrated by bundles of Sharpey's fibres aligned in concentric circles over the base surface (Figure 12.16).

The histological structure of the scales of *C. murchisoni* was described and illustrated by Gross (1947). The main features he noted were that there are up to 14 crown growth zones; the oldest growth zones lack ridges; the embryonic zone has wide semicircular canals and lacunae from which the dentine tubules radiate obliquely upwards and backwards, passing radially into the centre of each neck lamella; and arch-like connections extend between tubules in the upper neck posteriorly.

Our observations indicate that all growth zones, except the embryonic one, show ridges (Figure 13.1-3). As in all acanthodiforms, crown growth zones are superposed. Each zone is slightly wider in the neck than in the upper crown plane (Figure 13.1, 13.4), and all zones outside the embryonic one are of similar width (Figure 13.1, 13.2). Canals extend upwards and down into the base from the lacunae in the embryonic zone (Figure 13.6, 13.7). Eight radial canals extend from openings close to the neck-base rim towards the embryonic zone, with ascending canals rising up in the middle of each growth zone (Figure 13.4, 13.6,

13.8). The four posterior canals open out through small calibre canals on each side of the two neck protuberances (Figure 13.5). Ascending canals branch and form an irregular anastomizing network (Figure 13.7). Near the anterior edge of the scales, canals from the network in the neck turn sharply back horizontally, and are interconnected by a horizontal ring canal completely encircling each growth zone in the inner zones, and only along the anterior edge in the outer growth zones. Lacunae are formed at the junction of the canals. The horizontal canals lie under the grooves on the crown surface. Along the posterior sides of scales, the anastomizing networks forming the ascending canals gradually turn posteriorly and peter out into delicate dentine tubules reaching towards the surface of each growth zone. The central depression in the posterior surface of the crown of some scales appears to be related to a lower density of the networks of canals in this area of the scale. The central area of the upper plane in each crown growth zone is enameloid, with no dentine tubules visible. The base is formed of acellular bone lamellae. Sharpey's fibre bundles and canals of Williamson extend through the base (Figure 13.1-4). Scales in the proximal area of fin webs have a similar profile to the body scales, decreasing in size distally to scales with a low flat base with a thin elongate crown (Figure 13.9, 13.10). Thin fin rays, the 'ceratotrichia' of Miles (1970), underly the fin scales of each side of the web, apparently correlated one to one with the scales (Figure 13.10, 13.11). Being clearly overlain by normal scales, they are surely directly comparable with the endoskeletal ceratotrichia of chondrichthyans rather than the dermal lepidotrichia of actinopterygians.

Reconstruction: Our new observations on structures in the head and branchial regions of *Cheiracanthus murchisoni* are shown in Figure 14.

Cheiracanthus grandispinus McCoy, 1848

Figure 3, Figure 6.3-6.6, Figures 15-23

- | | |
|------|---|
| 1848 | <i>Cheiracanthus grandispinus</i> (M'Coy); M'Coy, p. 300. |
| 1855 | <i>Cheiracanthus grandispinus</i> (M'Coy); M'Coy, p. 582, pl. 2B, fig. 1. |
| 1860 | <i>Cheiracanthus grandispinus</i> ; Egerton, p. 123. |
| 1861 | <i>Cheiracanthus grandispinus</i> ; Egerton, p. 73. |
| 1888 | <i>Ch. grandispinus</i> , M'Coy; Traquair, p. 512. |
| 1890 | <i>Cheiracanthus grandispinus</i> ; Woodward and Sherborn, p. 29. |
| 1891 | <i>Cheiracanthus grandispinus</i> , M'Coy; Woodward, p. 20. |
| 1976 | <i>Cheiracanthus</i> spp. in part; Paton, p. 18. |
| 1979 | <i>C. grandispinus</i> M'COY 1848C; Denison, p. 47. |

TABLE 1. Comparison of total length, pectoral and dorsal fin spine lengths, scapulocoracoid height and minimum diameter for *Cheiracanthus* specimens in the NMS.

species	NMS G	fish length	pectoral spine length	dorsal spine length	scapula height	scapula minimum diameter
<i>Cheiracanthus grandispinus</i>	1893.107.9	220	40	40	12.5	2
<i>Cheiracanthus grandispinus</i>	1993.32.1	240	48	44	20	2
<i>Cheiracanthus grandispinus</i>	1973.12.105	240	38	34	18	2
<i>Cheiracanthus grandispinus</i>	1965.50.1	250	45	50	24	2.5
<i>Cheiracanthus grandispinus</i>	1893.107.10	250	-	50	-	-
<i>Cheiracanthus grandispinus</i>	1892.95.1	300	50	60	-	-
<i>Cheiracanthus grandispinus</i>	FR1938b	310	45	-	-	2.5
<i>Cheiracanthus latus</i>	1891.92.320	110	22.5	-	10	1
<i>Cheiracanthus latus</i>	1882.60.14	140	25	22	12	1.5
<i>Cheiracanthus latus</i>	1968.19.18	150	35	23	10	1
<i>Cheiracanthus latus</i>	1870.14.173	155	35	27	15	1.5
<i>Cheiracanthus latus</i>	1892.8.3	165	30	30	15	2
<i>Cheiracanthus purchisoni</i>	1965.59.34	100	17	17	6	<1
<i>Cheiracanthus purchisoni</i>	FR1369	120	19	17	9	1
<i>Cheiracanthus purchisoni</i>	1973.12.120	140	21	20	9	1
<i>Cheiracanthus purchisoni</i>	1891.92.307	150	22	22	9	1
<i>Cheiracanthus purchisoni</i>	1981.39.36	150	-	25	8	1
<i>Cheiracanthus purchisoni</i>	1870.14.171	150	27	22	9	1
<i>Cheiracanthus purchisoni</i>	1877.30.2	160	28	-	15+	1
<i>Cheiracanthus purchisoni</i>	FR1366	160	25	17	10	<1
<i>Cheiracanthus purchisoni</i>	1972.23.1	205	-	48	19	2
<i>Cheiracanthus purchisoni</i>	1898.163.4	205	-	23	10	-
<i>Cheiracanthus purchisoni</i>	1898.163.3	290	40	42	17	2
<i>Cheiracanthus purchisoni</i>	2000.65.2	110	20	20	7	1

? 1985 *Diplacanthus ? carinatus* in part; Valiukevičius, pl. 13.8.

1997 *C. grandispinus*; Young, p. 48.

2005 *Cheiracanthus grandispinus*; Newman and Dean, p. 3, 4.

2005 *C. grandispinus*; Newman and Dean, p. 4.

Holotype. SM H4423 from Orkney.

Material examined. From Marwick, Orkney: NMS G.2019.9.11. From Cruaday Hill quarry, Orkney: NMS G.2019.9.14; NMS G.2019.9.15; NMS G.2019.9.16. Orkney: NHMUK PV P.1363. From Achanarras: NMS G.1889.110.3; NMS G.1890.91.12; NMS G.1892.95.1; NMS G.1893.107.9; NMS G.1893.107.10; NMS G.1893.107.11; NMS G.1893.145.4; NMS G.1894.163.26; NMS G.1903.130.19; NMS G.1965.50.1; NMS G.1993.32.1; NMS G.2002.26.1481; NMS G.2019.9.2; NMS G.2019.9.4; NMS G.2019.9.5; NMS G.2019.9.6; NMS G.2019.9.7; NMS G.2019.9.9; NMS

G.2019.9.12; NMS G.2019.9.35; NMS G.FR1603; NMS G.FR1810; NMS G.FR1938; USCP F00130. From Clune: NMS G.1896.24.58. From Lethen Bar: NMS G.1891.92.317; NMS G.1864.7.12; NMS G.1966.40.24; NMS G.1973.12.105; NMS G.1973.12.106. From Gamrie: NMS G. 2019.9.3; NMS G.2019.9.4. From Jessie Port, Tarbat Ness Peninsula: NMS G.2019.9.8. From Cromarty: NMS G.2019.9.10; NMS G.2019.9.13. From Edderton: USCP F00115b. From the Moray Firth area: NMS G.1896.24.57.

Distribution. Sandwich Fish Bed Member to middle Upper Stromness Flagstone Formation (Eifelian), Orkney; Achanarras Fish Bed Member to upper Spital Flagstone Formation (Eifelian), Caithness; Nodule beds stratigraphically equivalent to the Achanarras Fish Bed Member, Moray Firth; Kernavė Regional Substage, eastern Baltic (upper Eifelian).

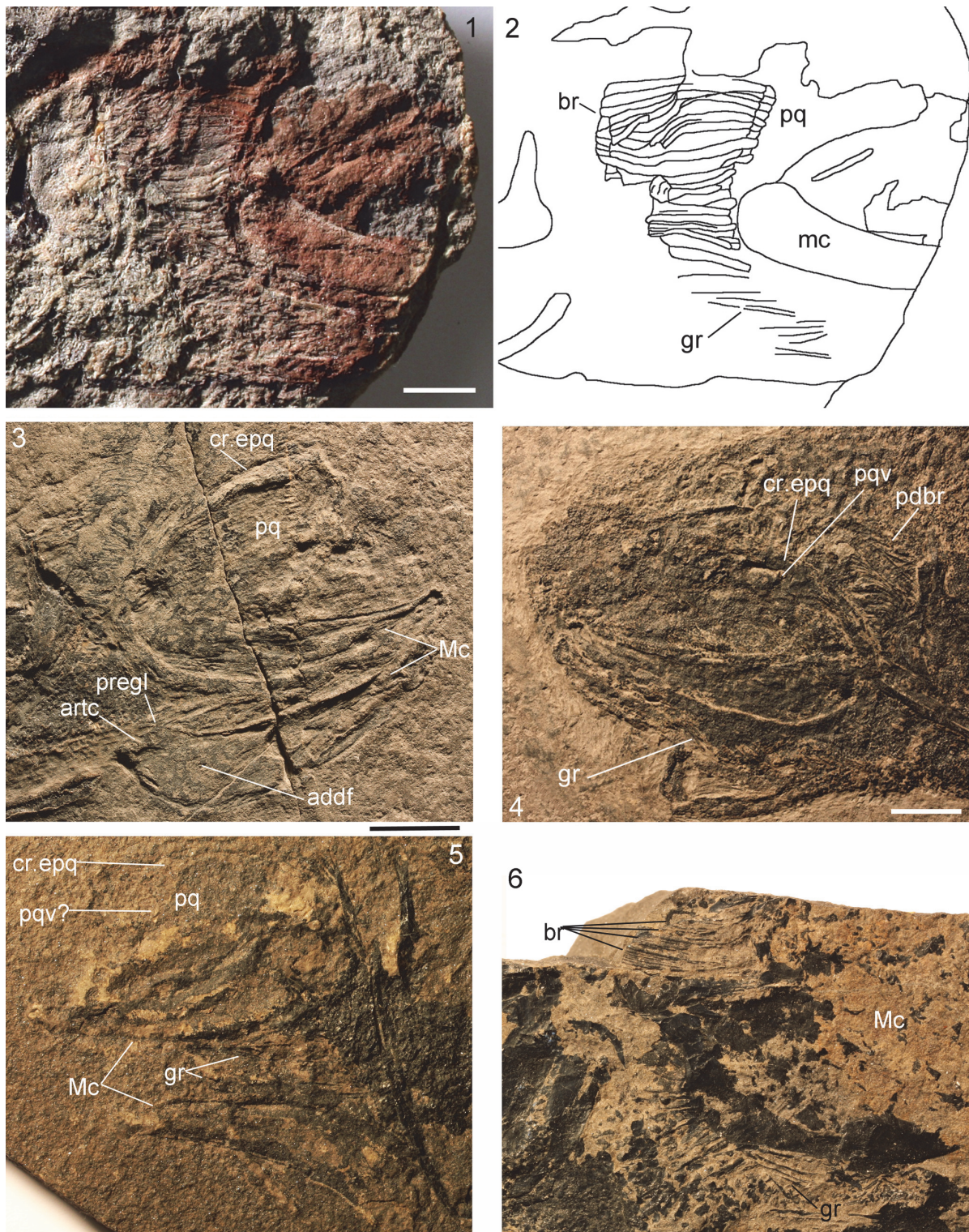


FIGURE 15. *Cheiracanthus grandispinus* head and branchial region, morphology. 1-2, NMS G.1966.40.24 from Lethen Bar. 3, NMS G. FR1603 from Achanarras Quarry, Caithness. 4, NMS G.2002.26.1481 from Achanarras Quarry. 5, NMS G.1903.130.19 from Achanarras Quarry, dorsoventrally flattened. 6, NHMUK PVP.1363 from Orkney. Scale bars equal 10 mm. addf, adductor muscle fossa; artc, articular cotylus; br, branchiostegal rays; cr.epq, extra-palatoquadrate ridge; gr, gular rays; Mc, Meckel's cartilage; pabr, posterodorsal branchiostegal rays; pq, palatoquadrate; pqv, palatoquadrate vacuity; pregl, preglenoid process. Anterior to right in 1-3, 6, to left in 4-5.

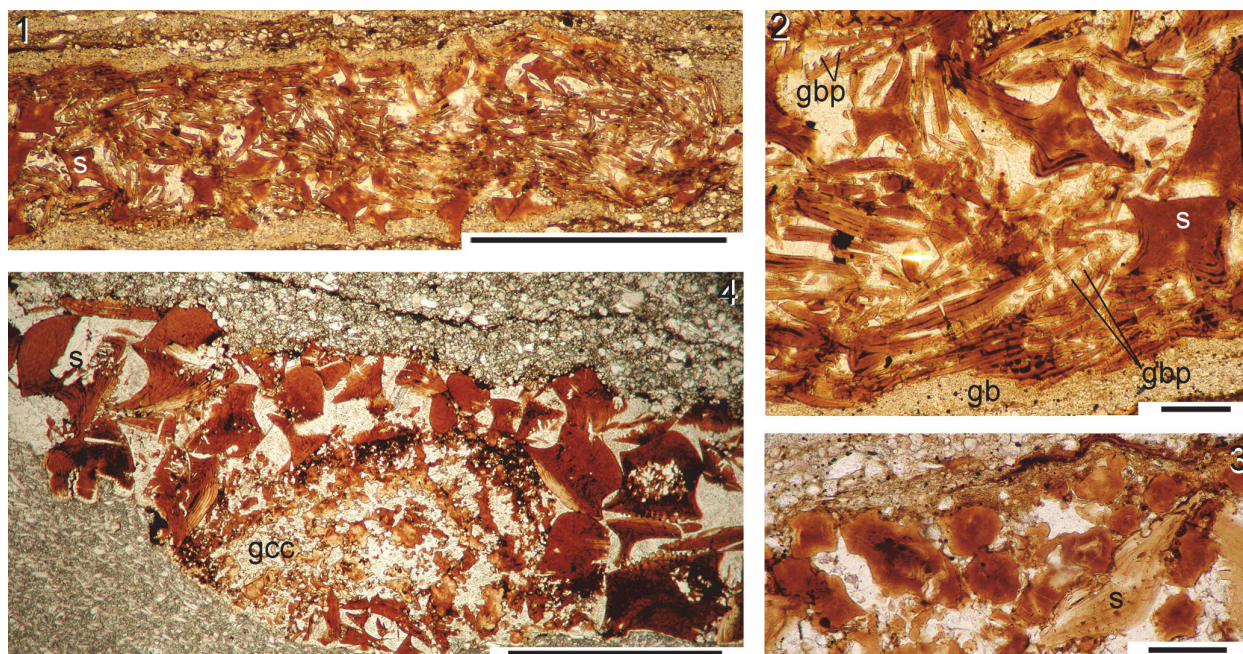


FIGURE 16. *Cheiracanthus grandispinus* head and branchial region, histology. 1-3, NMS G.2019.9.8: 1, 2, NMS G.2019.9.8.8 series of endoskeletal branchial rays, some showing gill raker projections; 3, NMS G.2019.9.8.14 calcified cartilage blocks; 4, NMS G.2019.9.35.1, calcified cartilage of Meckel's cartilage? Scale bars equal 0.1 mm. gb, gill bars; gbp, gill bar projections; gcc, globular calcified cartilage; s, scale.

Diagnosis. *Cheiracanthus* with Meckel's cartilage very deep at the posterior, maximum depth c. one-quarter length; scapula narrowest midshaft and widening dorsally and ventrally; branchiostegal rays broad, long, and ornamented with longitudinal ridges, with thinner rays dorsally, bending down at their posterior end; endoskeletal gill bars with short lateral projections; scale crown with marked smooth rim anteriorly, fan-shaped arrangement of ridges extending the length of crown, with narrow ridges curving away from a deep central groove posteriorly.

Description. General features. Presumed adult specimens of *C. grandispinus* are over 200 mm long, with the largest estimated to be up to 350 mm long (e.g., NMS G.FR1938A).

Head and branchial region: The jaw cartilages are similar to those of *C. purchisoni*, differing mainly in the greater relative depth of the Meckel's cartilage posteriorly (Figure 15.1-6). The maximum depth of the palatoquadrate is c. twice the maximum depth of the Meckel's cartilage. The fossa towards the posterior end for insertion of the adductor muscle extends about half the length of the jaw. The pre-glenoid process is quite rounded, and the articular cotylus is a narrow embayment of the usual form in acanthodians (Figure 15.3). The lateral face of the palatoquadrate has an extrapalatoquadrate ridge

(Figure 15.3-5) identical to that in *C. purchisoni*, as described by Watson (1937) and also has a vacuity in the same position as in *C. purchisoni* (Figure 15.4). The branchiostegal rays, with c. eight below the jaw articulation and c. 15 above, are quite broad and long, extending from the ventral edge of Meckel's cartilage to about midway up the posterior edge of the palatoquadrate (Figure 15.1, 15.2). The rays are ornamented with parallel longitudinal ridges (Figure 15.6). Long thin rays above the main branchiostegals are oriented obliquely, angled back and down with a downward turn at their posterior end (Figure 15.4). These are much more fragile than the branchiostegal rays and are rarely preserved. Numerous short, thin gular rays are present below the jaw line (Figure 15.1, 15.2, 15.4-6).

Notable histological features revealed by the thin sections through the branchial region are stacks of short mineralised endoskeletal elements that we identify as gill bars, or branchial rays, which we surmise to have extended out from the (unmineralised) branchial arches. Many of the gill bars in *C. grandispinus* have projections presumed to act as gill rakers on both sides (Figure 16.1, 16.2). This arrangement, with branchial rays extending out from the arches, is like that in modern chondrichthyans (cf. Gillis et al., 2009, p. 641),

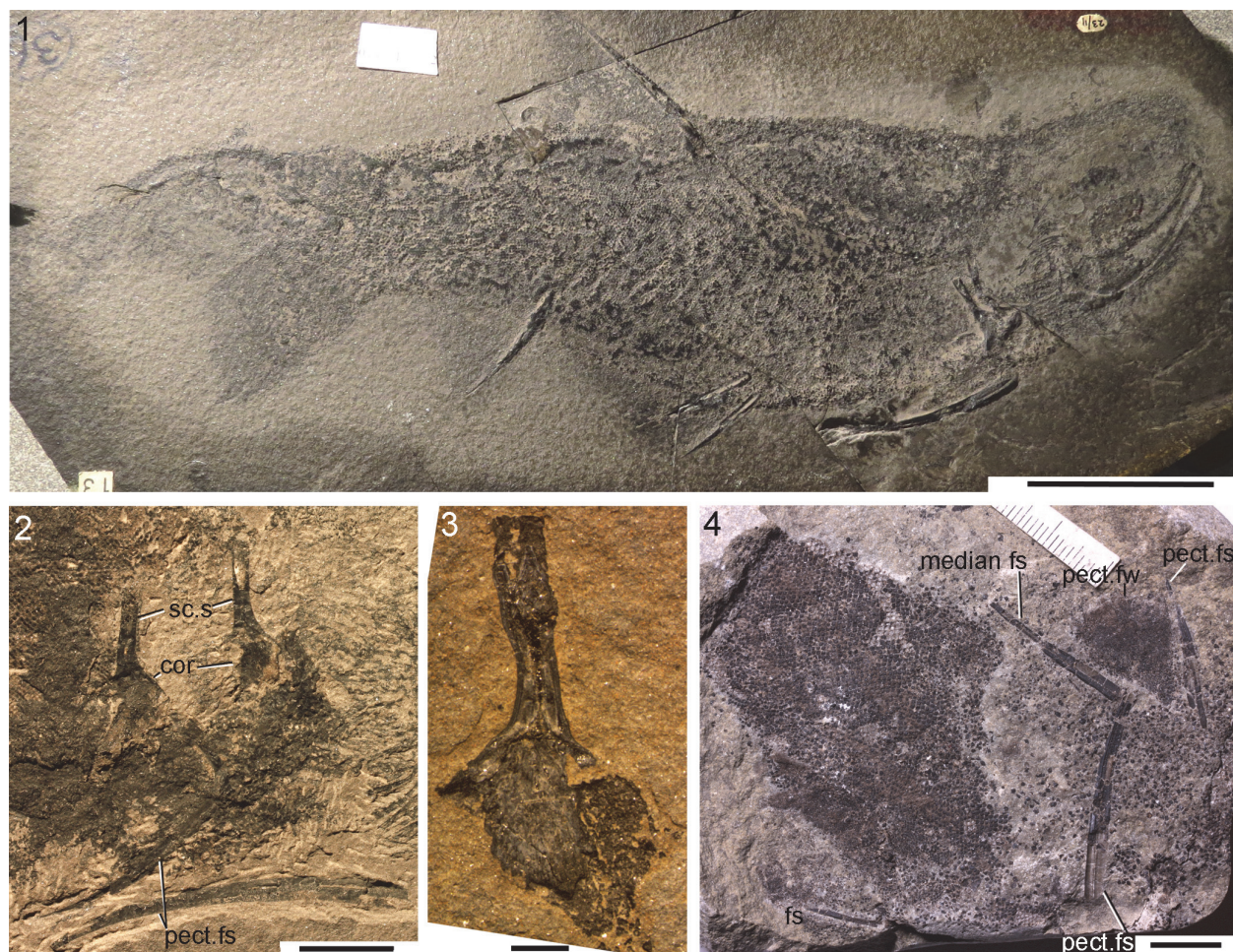


FIGURE 17. *Cheiracanthus grandispinus* pectoral region, spines morphology. 1, USCP F00130a from Achanarras, whole fish. 2, NMS G.FR1810 from Achanarras, scapulocoracoids and pectoral fin spines. 3, NMS G.2019.9.12, isolated scapulocoracoid from Achanarras. 4, disarticulated incomplete fish NMS G.2019.9.10.1 from Cromarty, ?two pectoral, one median (?dorsal), one pelvic spine. Scale bars equal 50 mm in 1, 10 mm in 3, 4, 2 mm in 2. cor, coracoid; fs, indeterminate fin spine, probably a pelvic; median fs, dorsal or anal fin spine; pect.fs, pectoral fin spine; pect.fw, pectoral fin web; sc.s, scapular shaft. Anterior to right.

rather than in the well-studied acanthodiform *Acanthodes*, which has separate robust gill rakers attached directly on the branchial arches (see Nelson, 1968, p. 139; Zidek, 1985, p. 156), and apparently lacks branchial rays. No mineralised gill bars were seen in the sacrificed specimen of *C. purchisoni*. The jaws are composed of blocky and globular calcified cartilage, as in *C. purchisoni* (Figure 16.3, 16.4).

Pectoral region and spines: The scapulocoracoid is more robust than that of *C. purchisoni*, with smallest diameter near the middle of the scapular shaft, and widening towards the dorsal end (Figures 3, 17.1-3). The coracoid height is equal to or greater than scapular height. A separate procoracoid was not preserved in any of the specimens examined. The spines show a similar morphology to those of

C. purchisoni, but the pectoral fin spines are slightly more robust (Figures 3, 17.1, 17.4). The dorsal spine is straight, positioned slightly behind the level of the pelvic spines, and has a basal cartilage (Figure 17.1).

Relative heights and widths of the leading edge ridge and body of spine vary depending on the spine position. In paired spines, the leading edge ridge is higher than wide; pectoral spines have an elongate leading edge ridge (Figures 18.1, 18.8-10, 19), and pelvic spines have a wide leading edge ridge (Figures 18.4, 18.5, 19). In median fin spines, this ridge is wider than high (Figure 18.6, 18.7). All spines, like those of other *Cheiracanthus* species, have a thin enameloid outer layer preserved on the leading edge ridge and the 'shoulders' (Figure 18.7-9). Spines have a wide central cavity

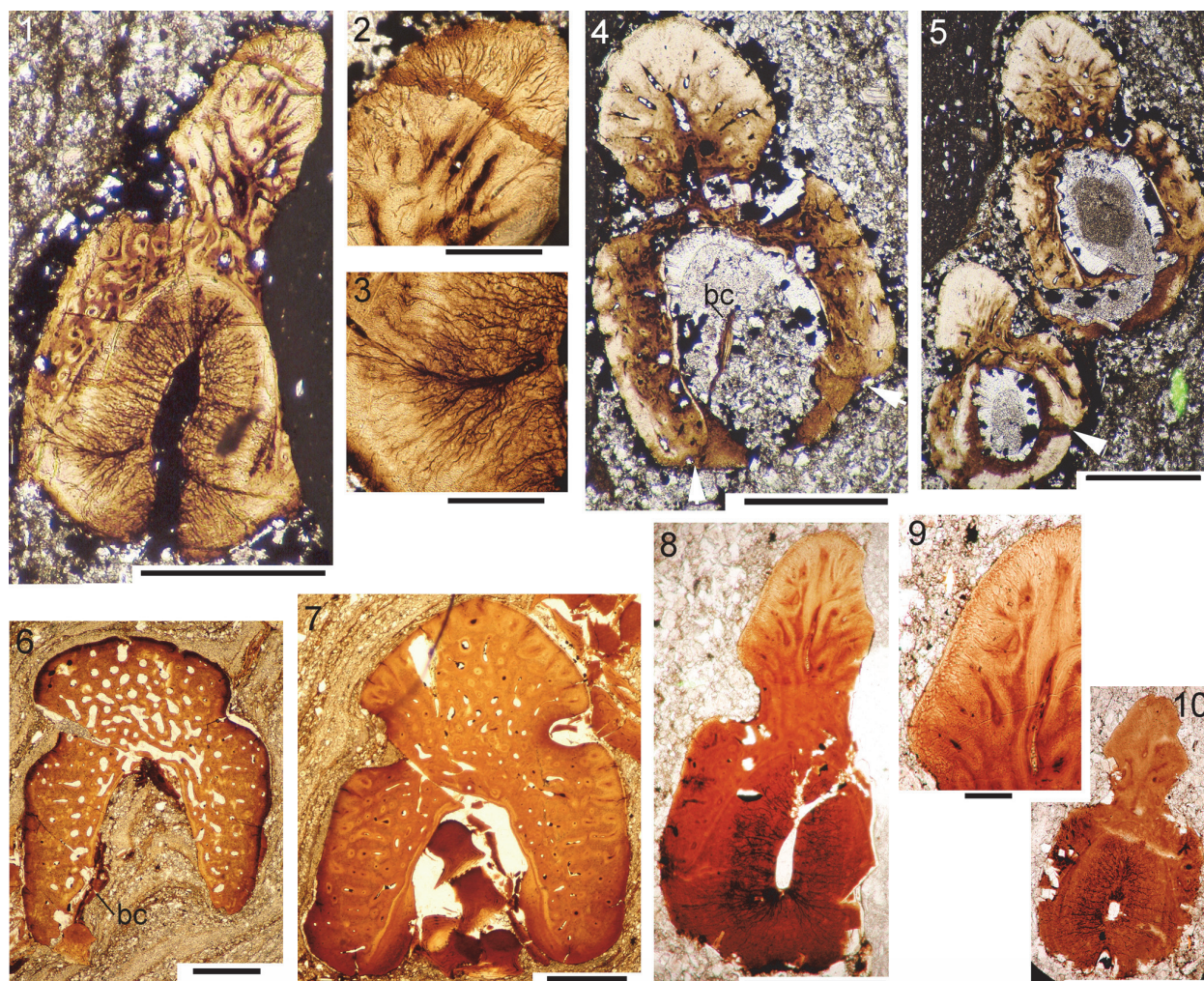


FIGURE 18. *Cheiracanthus grandispinus* spines histology. 1-5, NMS G.2019.9.7 from Achanarras: 1-3, NMS G.2019.9.7.21, thin section of distal end of pectoral spine, with closeups of the structure of the leading edge ridge and boundary between the main spine osteodentine and the areas bounding the trailing edge groove; 4, NMS G.2019.9.7.11, TS pelvic spine; 5, NMS G.2019.9.7.12, TS through both pelvic fin spines. 6, 7, NMS G.2019.9.8 from Jessie Port, median spine, ?anal: 6, TS NMS G.2019.9.8.8 at proximal end of exerted part; 7, NMS G.2019.9.8.15, towards mid spine. 8-10, NMS G.2019.9.35.1-7 from Achanarras, pectoral spine: 8, 9, NMS G.2019.9.35.2, midspine; 10, NMS G.2019.9.35.3, more distal. Scale bars equal 0.5 mm in 1, 4-8, 10, 0.1 mm in 2, 3, 9. bc, basal cartilage.

and lack an accessory pulp canal. Osteodentine forms most of the spine, with dentine tubules mostly only visible branching out towards the surface of the spine from the outermost longitudinal canals (Figure 18.2, 18.9). Longitudinal and interconnecting canals extend the length and breadth of the spine, with smaller canals leading off to open out in the sulcus between the leading edge ridge and the 'shoulders' of the spines (Figure 18.5), as well as into the central cavity (Figure 18.4, 18.6). Canals radiate out from the longitudinal canals in the leading edge ridge (Figure 18.2-5). Denteons are formed around the canals in the exerted part, but not in the inserted part. The inner lamellar layer

is present proximal to the closure of the central cavity (Figure 18.6, 18.7), and increases in thickness distally (Figure 18.1, 18.8, 18.10). Branching dentine tubules extend through each of the lamellar layers, perpendicular to the inner surface (Figure 18.1, 18.3). In the Achanarras preservation type (Figure 18.1-5), a clear boundary is visible between the denser tissue of the posterior face of the spine and the osteodentine and inner lamellar layers of the main body of the spine. Remnants of a separate thin layer of tissue lining part of the central cavity are preserved towards the proximal end in some of the spines (Figure 18.4, 18.6, 18.7).

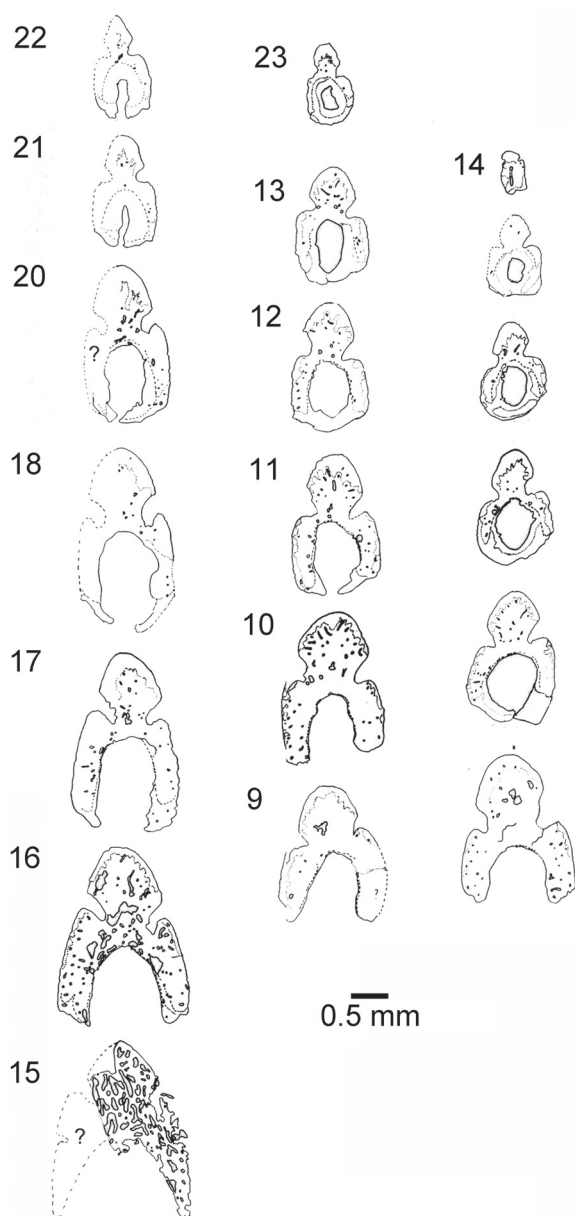


FIGURE 19. *Cheiracanthus grandispinus* NMS G.2019.9.7, serial sections of pectoral (22-15) and pelvic (9-14, 23) spines, thin section drawings, numbered as on map in Figure 6.4.

Body scales: Scales of larger fish (200 mm or more long) are easily distinguishable from scales of other species of *Cheiracanthus*, with a fan-shaped arrangement of crown ridges anteriorly (Figure 20.1-6), and with the ridges curving away from a deep central groove posteriorly in the midline. Even in the fin web scales (Figure 20.7-9), the same fan-shaped pattern is visible. The crown is up to 1.5 mm long on flank scales (Figure 20.6) and usually longer than wide. The crown ridges are

narrow but vary slightly in width, apparently randomly, and extend the whole length of the crown (Figure 20.10, 20.11). Particularly on worn scale crowns, the ornament more resembles grooves cut into the crown, rather than ridges developed above the crown plane (Figure 20.13-17). Broad low longitudinal swellings line the median groove. Extra ridges are developed laterally in the posterior half of the crown, usually at a slightly lower level than the central crown (Figure 20.10, 20.11, 20.14, 20.15). A broad smooth rim is present in front of the ridges along the anterior edge. In scales from smaller, presumed juvenile fish, and in the older growth zones, crown ridges are more radially arranged, extra lateral ridges are lacking, and the postero-lateral edges are sometimes serrated. This morphology is visible on primordial scale crowns exposed through flaking off of overlying growth zones (Figure 20.5). The surface of the crown in all scales is convex both longitudinally and side to side. The neck and base are developed similarly to those in *C. murchisoni*, with a neck that is as deep or deeper than the base, and a pair of protuberances posteriorly (Figure 20.12, 20.13, 20.16-18).

In many aspects, the histological structure of the scales is similar to that of *C. murchisoni*. The embryonic zone (primordial scale) has large lacunae interconnected by short narrow canals, with other short canals extending upwards and down towards the base cone (Figure 21.1-4). The crown surface of the primordial scale is concave in longitudinal and transverse sections. In younger zones the surfaces become more and more convex both longitudinally and transversely (Figure 21.1-9). The deep median longitudinal groove extends through all the zones in the posterior half of the scale (Figure 21.4).

As in *C. murchisoni*, eight regularly spaced, radial canals extend through the lower crown (Figure 21.9, 21.10), with anastomizing networks of ascending canals running up in each crown growth zone (Figure 21.4-8). The junction between the posterior radial and ascending canals shows a wide lacuna in the younger growth zones. Anteriorly, the ascending canals are interconnected in a ring canal consisting of short, arched tubules before turning back horizontally (Figure 21.11, 21.12). In young individuals and juvenile growth stages, each groove between the more lateral ridges is usually underlain by only one horizontal canal, and the ridges appear gently rounded in cross section. With growth of the scales the younger ridges show a more flat-topped shape,

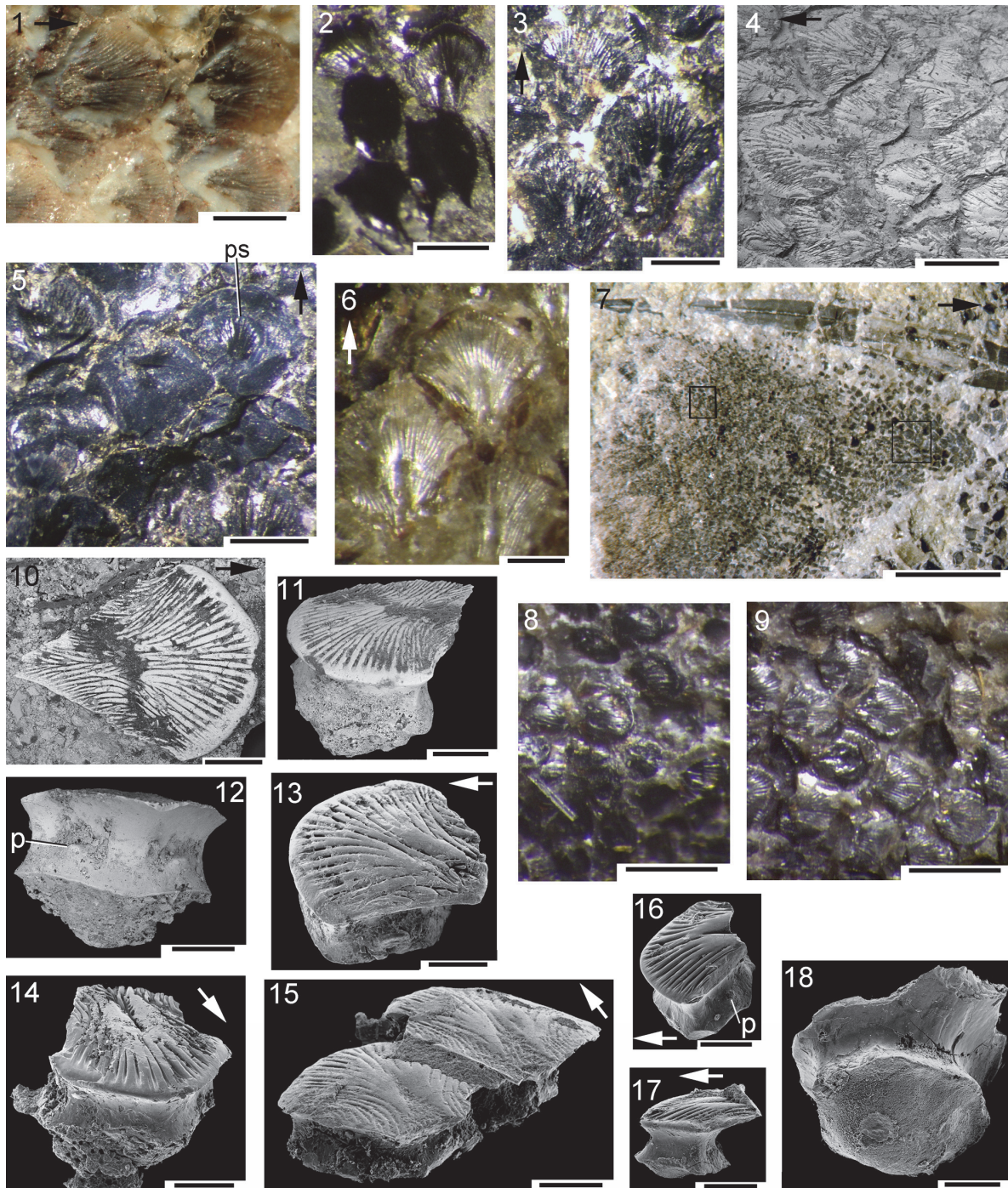


FIGURE 20. *Cheiracanthus grandispinus* scale morphology. 1-3, 5-9, light microscope images; 4, 10-18, SEM images; midbody scales unless detailed otherwise. 1, NMS G.1891.92.317 from Lethen Bar. 2, NMS G.2019.9.8 from Jessie Port, Ross and Cromarty. 3, 4, USCP F00115b from Edderton. 5, NMS G.2019.9.9 from Achanarras, primordial scale revealed after abrasion/flaking of overlying crown growth zones. 6-9, NMS G.2019.9.10.1 from Cromarty: 6, mid-body scales; 7-9, pectoral fin web: spine and web; 8, distal scales; 9, scales near fin base. 10-12, NMS G.2019.9.11 from Marwick: 10, view of crown before removal of scale from matrix; 11, anterocrown view; 12, posterior view. 13, NMS G.2019.9.3.27.1 from Gamrie Den of Findon, laterocrown view. 14-18, NMS G.2019.9.13.8 from Cromarty, Eathie to Navity: 14, NMS G.2019.9.13.8.16, anterocrown view; 15, NMS G.2019.9.13.8.2 pair of scales in posterocrown view; 16, NMS G.2019.9.13.8.8, laterocrown view; 17, NMS G.2019.9.13.8.6, lateral view; 18, NMS G.2019.9.13.8.17, posterobasal view. Scale bars equal 0.5 mm in 1-9, 0.2 mm in 10-18. p, neck protuberance; ps, primordial scale. Arrows indicate anterior.

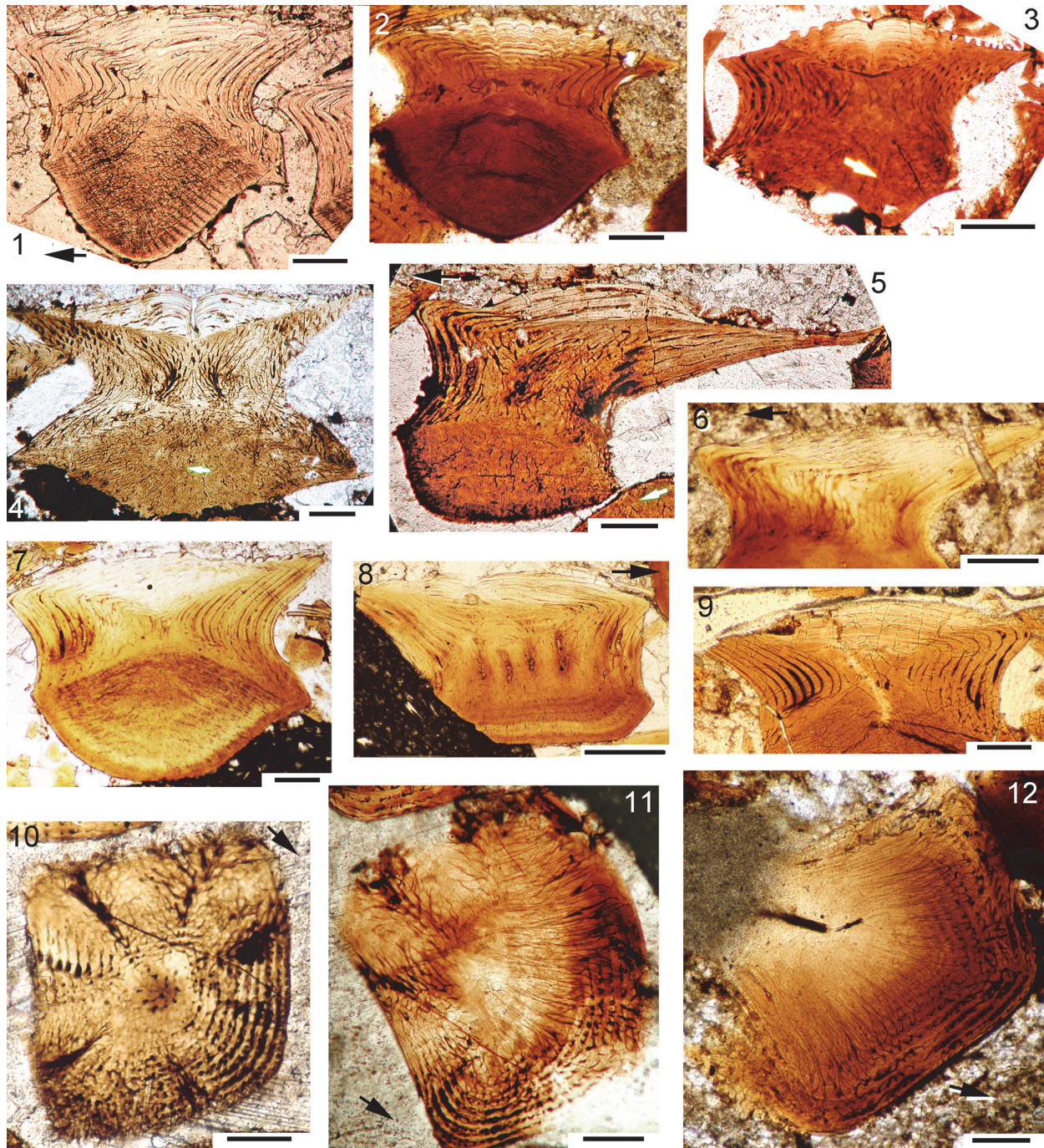


FIGURE 21. *Cheiracanthus grandispinus* scale histology. 1, NMS G.2019.9.3.9 from Gamrie, vertical longitudinal section through posterior protuberance. 2, 9, 12, NMS G.2019.9.8 from Jessie Port, Ross and Cromarty: 2, NMS G.2019.9.8.14, anterior crown vertical transverse section; 9, NMS G.2019.9.8.10, crown vertical transverse section; 12, NMS G.2019.9.8.13, crown horizontal section. 3, NMS G.2019.9.35.6, from Achanarras, midscale vertical transverse section. 4, 5, 10, 11, from Achanarras: 4, NMS G.2019.9.2.4, posterior half of scale, vertical transverse section; 5, NMS G.2019.9.2.2, vertical longitudinal section; 10, NMS G.1893.107.9.2, horizontal section through crown base; 11, NMS G.1893.107.9.2, horizontal section through midcrown. 6-8, NMS G.2019.9.10 from Cromarty: 6, NMS G.2019.9.10.3, off-centre vertical longitudinal section; 7, NMS G.2019.9.10.5, vertical transverse section; 8, NMS G.2019.9.10.9, oblique vertical section through side of scale. Scale bars equal 0.1 mm. Arrows indicate anterior.

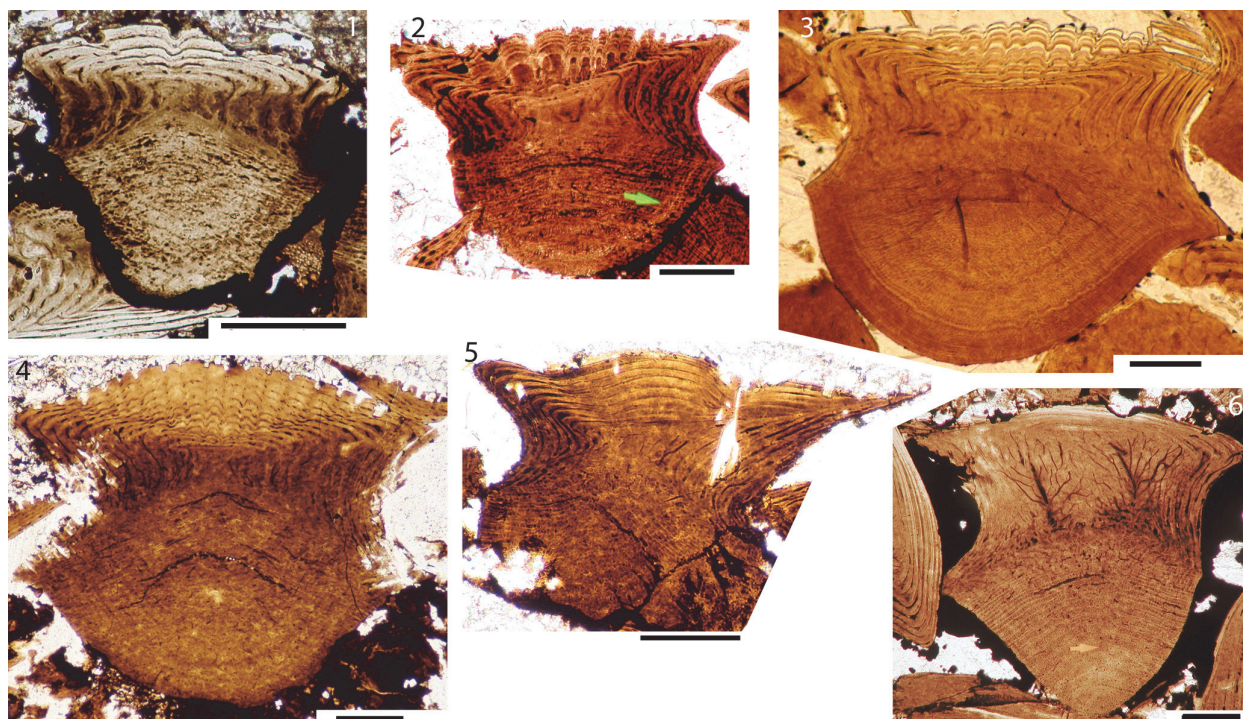


FIGURE 22. *Cheiracanthus grandispinus* comparison of scale structure in different sized fish. 1, NMS G.2019.9.5.2, from Achanarras, small fish c. 10 cm long, vertical transverse section through scale anterior. 2, NMS G.2019.9.6.1, from Achanarras, medium sized fish less than 30 cm long, vertical transverse section through scale anterior. 3, NMS G.2019.9.8.12, from Jessie Port, medium sized fish, vertical transverse section through scale anterior. 4, NMS G.2019.9.9.14, from Achanarras, fish 30 cm or longer, vertical transverse section through scale anterior. 5, NMS G.2019.9.9.7, from Achanarras, fish 30 cm or longer, vertical longitudinal section. 6, NMS G.2019.9.35.4, medium sized incomplete fish, vertical section of scale showing Sharpey's fibre bundles through base. Scale bars equal 0.1 mm.

and the grooves are underlain by two to four canals which sometimes intertwine (Figure 21.11, 21.12). More posteriorly, regularly placed dentinal tubules run off the canals into the ridges, sometimes forming a network between adjacent ridges. Enameloid fills most of the upper plane in each crown growth zone, with longitudinal dentine tubules near the base of each zone (Figure 21.1-9). Sharpey's fibre bundles in the base are wider than those of *C. mur-*

chisoni, so the isopedin-like layering of the sheets of fibres (Figure 21.1, 21.7) appears coarser than in that species. Otherwise, the bases resemble those of *C. purchisoni*.

The number of crown growth zones increases as the size of the fish increases (Figure 22.1-4). Up to seven crown growth zones were noted in scales of the smallest fish, which was about 100 mm long (Figure 22.1), and up to 15 in the largest fish sampled, which were over 300 mm long (Figure 22.4, 22.5).

Reconstruction: Our observations of structures in the head to pectoral region of *Cheiracanthus grandispinus* are shown in Figure 23.

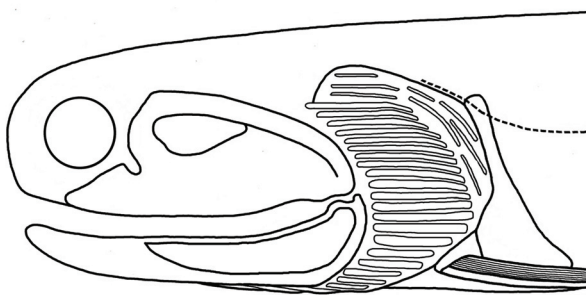


FIGURE 23. *Cheiracanthus grandispinus* head and branchial region reconstruction.

Cheiracanthus latus Egerton, 1861
Figure 4, Figure 6.5-6.8, Figures 24-32

- 1861 *Cheiracanthus latus*; Egerton, 73-75, pl. 10.
- 1888 *Ch. latus*, Egerton; Traquair, p. 512.
- 1890 *Cheiracanthus latus*; Woodward and Sherborn, p. 29.
- 1891 *Cheiracanthus latus*, Egerton: Woodward, p. 19
- 1937 *Cheiracanthus latus* Eg.; Watson, p. 88, fig. 13, pl. 12, figs. 4-6.

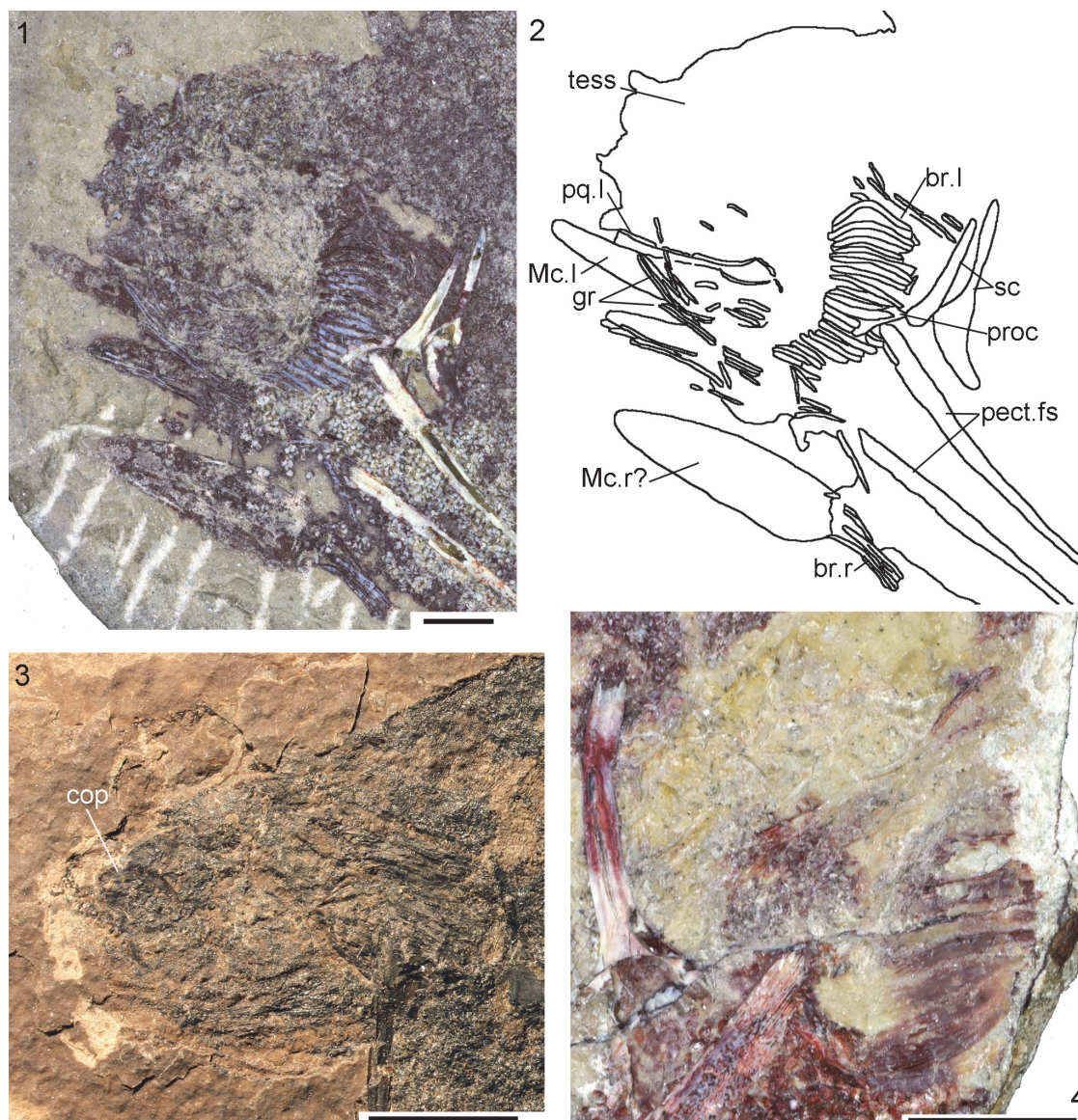


FIGURE 24. *Cheiracanthus latus* head and branchial region, morphology. 1-2, NHM PV P 3253 from Tynet Burn. 3, NMS G.1891.92.320 from Gamrie. 4, NHMUK PVP43273 from Tynet Burn, branchial region with ridges visible on lowest branchiostegal plates. Abbreviations: br.l, left branchiostegal plates; br.r, right branchiostegal plates; cop, circumorbital plate; gr, gular rays; Mc.l, left Meckel's cartilage; Mc.r, right Meckel's cartilage; pect.fs, pectoral fin spines; pq.l, mineralised cartilage along ventral edge of left palatoquadrate; proc, procoracoid; sc, scapulocoracoids; tess, head tesserae. Scale bars equal 10 mm.

- 1947 *Cheiracanthus latus* Egerton; Gross, p. 125-126, fig. 13G, pl. 25, fig. 4.
 1966 *Cheiracanthus latus* Egerton; Miles, p. 157, 159, fig. 6A, 8E.
 1970 *Cheiracanthus latus* Egerton; Miles, p. 349, 358, 362.
 1973 *Cheiracanthus latus* Egerton; Miles, p. 157, text-fig. 22.
 1973 *Cheiracanthus longicostatus*; Gross, p. 69, figs. 33E, 34A-C, pl. 28.16-20.

- ? 1973 *Cheiracanthus brevicostatus* in part; Gross, pl. 28.12.
 1976 *Cheiracanthus latus*; Zidek, p. 23.
 1976 *Cheiracanthus* spp. in part; Paton, p. 18.
 1979 *Cheiracanthus latus*; Denison, figs. 29F, 30B, 31A-C.
 1979 *C. latus* Egerton 1861B; Denison, p. 47.
 1985 *Cheiracanthus longicostatus*; Valiukevičius, p. 35, figs. 12-14, plates 2.1-10, 4.10-11, 8.7-8, 10, 11.10.

- 1988 *C. longicostatus*; Valiukevičius, p. 75.
 1995 *Cheiracanthus longicostatus*; Valiukevičius, Talimaa and Kruchek, figs. 1-5.
 1995 *Cheiracanthus latus*; Young, p. 68, fig. 8.
 1996 *Cheiracanthus latus*; Gagnier, p. 162.
 1997 *C. latus*; Young, p. 48.
 1999 *C. latus* Egerton, 1861; Dineley and Metcalf, ch. 6, Den of Findon p. 3.
 1999 *Cheiracanthus latus* Egerton, 1861; Dineley and Metcalf, ch. 6, Tynet Burn p. 4, fig. 6.20A.
 2000 *Cheiracanthus longicostatus* Gross; Valiukevičius, figs. 1, 4, 5.
 2002 *Cheiracanthus longicostatus* [sic]; Valiukevičius, table 1.
 2002 *Cheiracanthus longicostatus*; Valiukevičius, p. 37.
 2005 *C. latus* Egerton, 1861; Burrow and Young, p. 13.
 2005 *Cheiracanthus latus*; Burrow and Young, p. 15.
 2009 *Cheiracanthus latus*; Albert et al., app. 1 p. 371.
 2010 *Cheiracanthus longicostatus*; Sallan and Coates, p. 24.
 2011 *Cheiracanthus latus*; Retallack, fig. 1C.
 2014 *Cheiracanthus longicostatus*; Ivanov and Märss, p. 158.
 ? 2015 *Cheiracanthus longicostatus*; Plax, pl. 4, figs. 3, 4.
 2018 *C. latus* Egerton; Glinskiy and Pinakhina, p. 84.
 2018 *Cheiracanthus latus*? Egerton; Pinakhina and Märss, p. 99, table 1, fig. 4R.
 2019 *Cheiracanthus latus* Egerton, 1861; Newman, Burrow and den Blaauwen, p. 13, figs. 13, 14.

Holotype. NHM UK PV P3253 from Tynet Burn.

Remarks. Egerton (1861, pl. 10) states that the type specimen figured by him was forwarded to him by the then recently deceased Duke of Richmond, from his quarries at Tynet Burn. This specimen is not part of the Egerton collection now in the Natural History Museum and therefore must be considered lost. However, it is known that Egerton and his good friend William Cole, 3rd Earl of Enniskillen, used to swap parts and counterparts with one another (E. Bernard, pers. comm.) As NHM UK PV P3253 is part of the Enniskillen collection (also housed in the NHMUK) and is a mirror image of Egerton's (1861, pl. 10) figure, it is certain that it is the counterpart of Egerton's (1861) type specimen and is therefore one half of the holotype.

Material examined. From Cromarty: NMS G.1870.14.145. From Cushnie Burn: NMS G.1965.59.38. From Gamrie: NMS G.1870.14.173; NMS G.1882.60.14; NMS G.1891.92.320; NMS G.1892.8.3; NMS G.1891.92.320; NMS G.2019.3.7; NMS G.2019.9.19; NMS G.22019.9.22; NMS

G.2019.14.7; NMS G.2019.14.8. From Tynet Burn: NHM UK PV P3253a [note: not the counterpart of the holotype]; NHM UK PV P43273a, b; NMS G.1968.19.18; NMV P29280; NMV P203744; NMV P204033; QMF60004 From Jessie Port, Tarbat Ness Peninsula: NMS G.2019.3.3. From Geanies Point, Tarbat Ness Peninsula: NMS G.2019.9.17; NMS G.2019.9.18; NMS G.2019.14.9; NMS G.2019.9.20; NMS G.2019.9.23; NMS G.2019.14.4. From Hilton of Cadboll (below the Achanarras horizon): NMS G.2019.14.10. From Eathie, Black Isle: NMS G.2019.9.21. From Tarrel Bay, Tarbat Ness Peninsula: NMS G.2018.28.26.

Distribution. Nodule beds stratigraphically equivalent to the Achanarras Fish Bed Member (Eifelian), Moray Firth; Narva (Narova) Formation (Eifelian), Estonia, Latvia, and Narva R.S. Russia, possibly ranging from the Rezekne R.S. (upper Emsian) to the top of the Burtneki R.S. (upper Givetian) in the Baltic countries and Belarus (Valiukevičius, 2000; Plax, 2015).

Diagnosis. *Cheiracanthus* with large deep tail, its greatest depth c. one-third the length of the fish; deep palatoquadrate with maximum depth c. 2.5 times maximum depth of Meckel's cartilage; Lunate dorsal circumorbital bone; dorsal branchiostegal rays very short and slender with a distinct bend downwards on their anterior ends; long, thin rays above the main branchial cover; scale crowns with two broad median ridges edging median longitudinal sulcus with an oval pit in the posterior half; posterior crown with serrated margin.

Description. General features: The body shape and relative proportions of the fins were described by Watson (1937). The most obvious feature distinguishing *C. latus* from *C. purchisoni* and *C. grandispinus* is the large caudal fin. The dorsal spine is slender and straight, positioned midway between the levels of the pelvic and anal spines. The anal spine is also slender and straight, and c. 80% the length of the dorsal spine. The pelvic spines show a very slight curvature, and are c. 65% the length of the dorsal spine. The pectoral spines are a similar length to the dorsal spine and slightly curved.

Head and branchial region: The head of *Cheiracanthus latus* is very similar to that of *Cheiracanthus purchisoni*. The only difference Watson (1937) noted was that the dorsalmost branchiostegal rays in *C. latus* are shorter, slenderer, and the anterior ends turn sharply ventrally (Figure 24.1, 24.2). We note that the main branchiostegal rays are ornamented with thin parallel longitudinal ridges, however, this ornament is

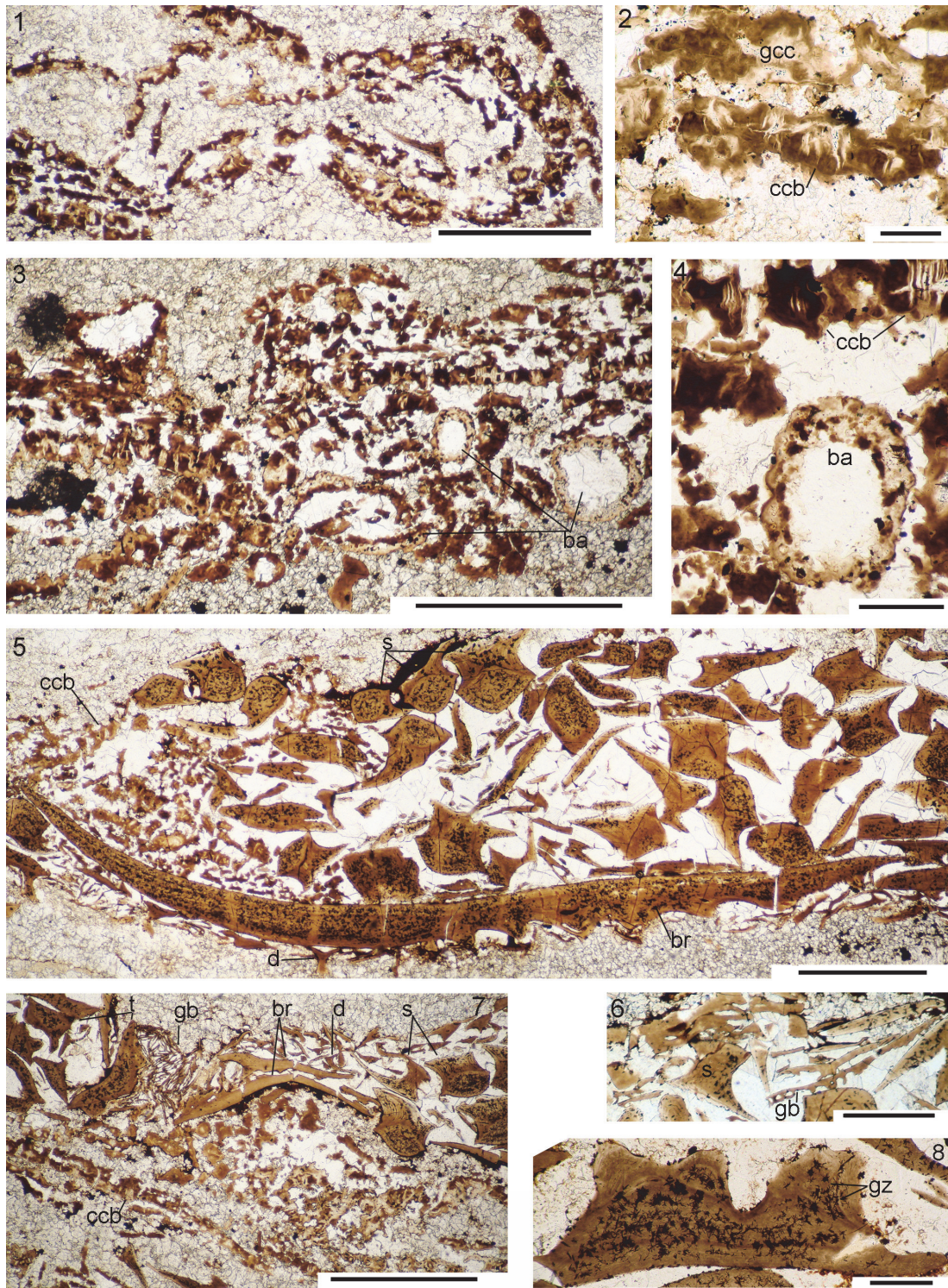


FIGURE 25. *Cheiracanthus latus* head and branchial region, histology, NMS G.2019.3.3; position of sections shown in Figure 6.6. 1, 2, thin section NMS G.2019.3.3.3: 1, ?Meckel's cartilage; 2, closeup of calcified cartilage blocks; 3, 4, NMS G.2019.3.3.5, indet. jaw cartilage and branchial arches; 5, NMS G.2019.3.3.2, branchiostegal plate in oblique section, body scales, branchial denticles, indet. cartilage; 6, NMS G.2019.3.3.4, body scales, gill bars; 7, 8, NMS G.2019.3.3.17: 7, jaw cartilage, head tesserae, gill bars, branchiostegal plates; 8, head tessera vertical section, stellate mineralisation artifacts. Scale bars equal 1.0 mm in 1, 3, 5, 7, 0.1 mm in 2, 4, 6, 8. ba, branchial arch; br, branchiostegal plate; ccb, calcified cartilage blocks; d, denticle; gb, gill bar; gcc, globular calcified cartilage; gz, growth zones in crown; s, body scale; t, tessera.

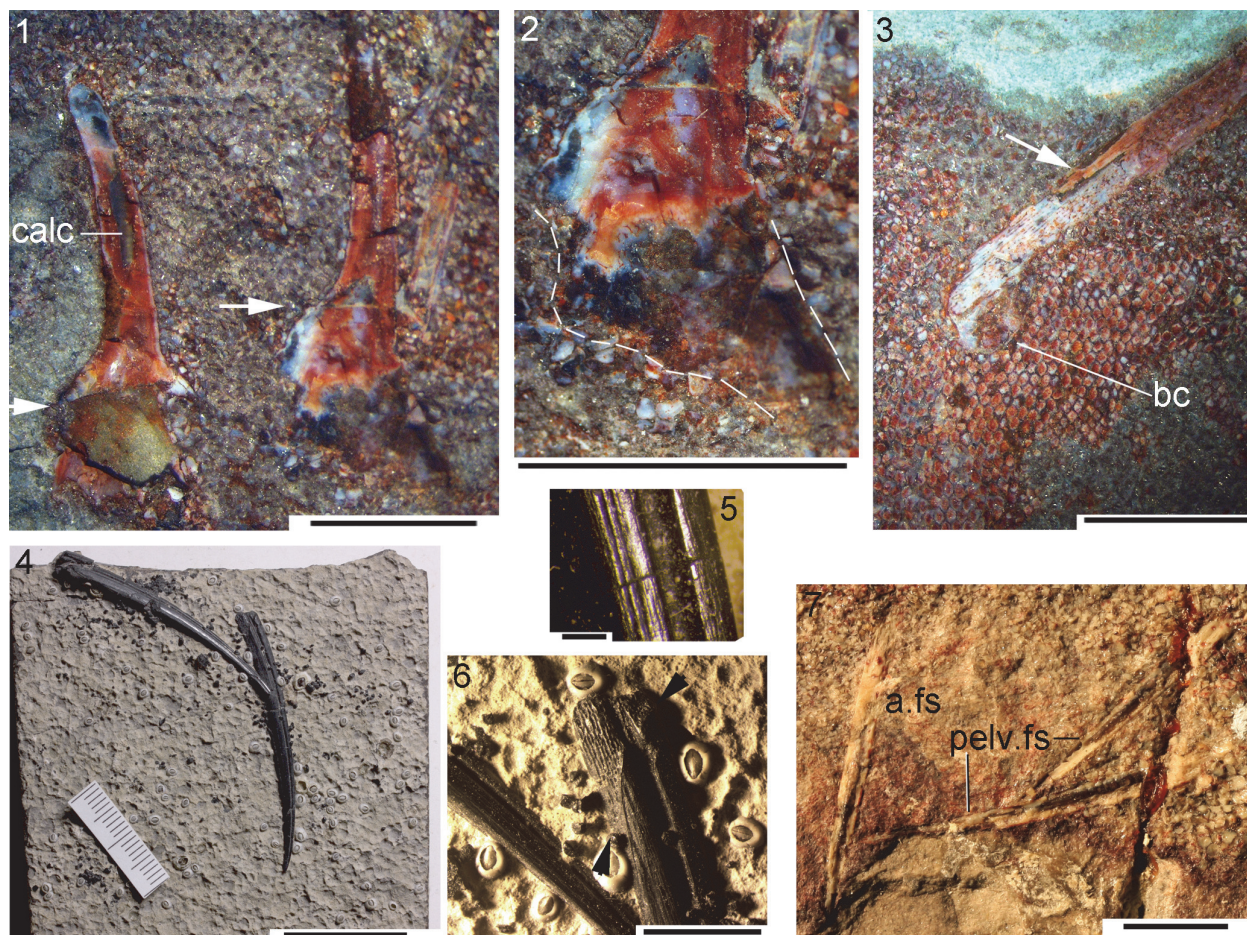


FIGURE 26. *Cheiracanthus latus* pectoral region and spines, morphology. 1-3, QMF60004 from Tynet Burn: 1, left and right scapulocoracoids, white arrows indicate separation between scapula and coracoid; 2, close up of right coracoid shape (dotted line); 3, dorsal fin spine insertion and basal cartilage, white arrow indicates insertion/exertion boundary. 4-6, NMS G.2018.28.26 from Tarrel Bay: 4, left and right pectoral spines as collected; 5, closeup of thin ridges on lateral or medial? side of right spine; 6, insertion area of right spine. 7, NMS G.1968.19.18, anal and pelvic spines. Scale bars equal 5.0 mm in 1-3, 6, 20 mm in 4, 7, 0.5 mm in 5. a.fs, anal fin spine; bc, basal cartilage; calc, calcite infill; pelv.fs, pelvic fin spines.

rarely seen as the rays usually fracture centrally when nodules are split. NHM P43273 is a rare specimen where it is visible (Figure 24.4). We also note that *C. latus* has distinct circumorbital bones (Figure 24.3) with the most dorsal one extending about one-fifth the circumference of the orbit.

Thin sections (Figure 25) show that the jaws and most other endoskeletal structures in these regions are mineralised as calcified cartilage (cc) with the same basic varieties as in *C. murchisoni*. The jaws are mostly a single layer of contiguous calcified cartilage blocks (Figure 25.1-3), and the branchial arches comprise a more irregular consolidated globular calcified cartilage forming cylinders filled with calcite that has presumably replaced the uncalcified cartilage core. The endoskeletal branchial arches show a similar structure as in *C. mur-*

chisoni, but the walls are thinner and appear to comprise only one layer (Figure 25.3, 25.4). As the *C. latus* fish sacrificed for thin sectioning was larger than the *C. murchisoni* one, it is unlikely that the difference in thickness is related to the size of the fish. The dermal branchiostegal plates and smaller gular rays are formed of a dense lamellar bone (Figure 25.5-7); the ornament layer on the branchiostegal rays comprises sharp crested ridges. Small mono- and multicupid denticles are preserved around the branchiostegal rays (Figure 25.5, 25.7). Blocks of short, thin mineralised elements within the branchial regions are interpreted as the endoskeletal gill bars (Figure 25.6, 25.7); some show short projections (Figure 25.6). Flat or concave based dermal tesseræ from the head region have a lamellar base and areal-growth



FIGURE 27. *Cheiracanthus latus* pectoral region and spines, histology. 1-6, NMS G.2019.3.31 (see Figure 6.6 for map of sections): 1, slice II before grinding (corresponds to sections 6, 7), arrow indicates dorsal direction; 2, NMS G.2019.3.3.7, scapulocoracoid, long section mid-shaft; 3, NMS G.2019.3.3.12, TS pectoral spine at insertion/exertion boundary; 4, NMS G.2019.3.3.10, TS of spine close to insertion; 5, NMS G.2019.3.3.6, close up of leading edge ridge structure of pectoral spine, midspine; 6, NMS G.2019.3.3.2, TS pectoral spine near the tip. 7-10, NMS G.2018.28.26, TS pectoral spines: 7, 2018.28.26.9, close to insertion; 8, 2018.28.26.7, midspine; 9, 10, 2018.28.26.5, towards tip, with closeup of infilling dentine. 11-14, NMS G.2019.3.7 TS pectoral spine, near insertion, and flange of scapulocoracoid: 11, NMS G.2019.3.7.8; 12, NMS G.2019.3.7.9; 13-14, NMS G.2019.3.7.10, outer side of spine with thin sharp ridges. Scale bars equal 10 mm in 1; 0.1 mm in 2, 5, 10; 0.5 mm in 3, 4, 6, 7-9, 11-14. c.cav, central cavity; ccb, calcified cartilage blocks; dt, dentine tubules; en, enameloid; l.pect.fs, left pectoral fin spine; min, stellate mineralisation; ost, osteodentoon; pect.fs, pectoral fin spine; r, ridges; s, scale; sc, scapulocoracoid.

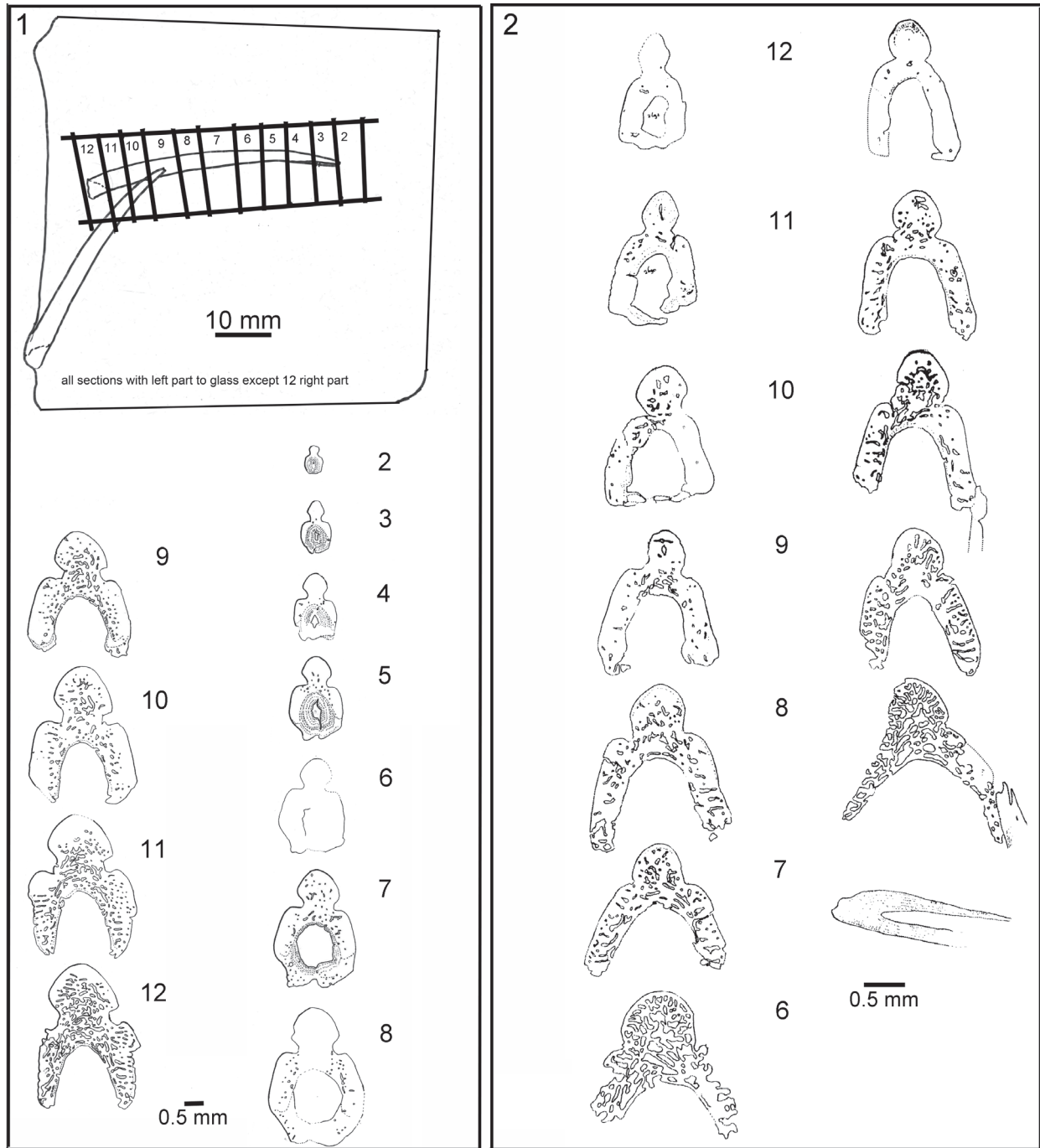


FIGURE 28. *Cheiracanthus latus* pectoral spines, serial transverse section drawings. 1, NMS G.2018.28.26 (see Figure 27): sketch map and drawings of each section. 2, NMS G.2019.3.7 (see Figure 6.7, 8): sections NMS G.2019.3.7.6-12 through pectoral spines and scapulocoracoid.

odontodes formed of acellular layered dentine (Figure 25.7, 25.8).

Pectoral region and fin spines: The scapulocoracoid of *Cheiracanthus latus* closely resembles that of *C. purchisoni*, with a slender tapering scapular shaft (Figures 24.1-4, 26.1). Miles (1973, text-figure 22) described the pectoral region of *C. latus*,

correcting some of the observations made by Watson (1937). We note that there is a marked delimitation between the scapula and the coracoid ossifications (Figure 26.1-2).

None of the fin spines are deeply inserted, contra Watson (1937). As noted by Watson (1937), the dorsal fin spine has a basal bone (Figure 26.3);

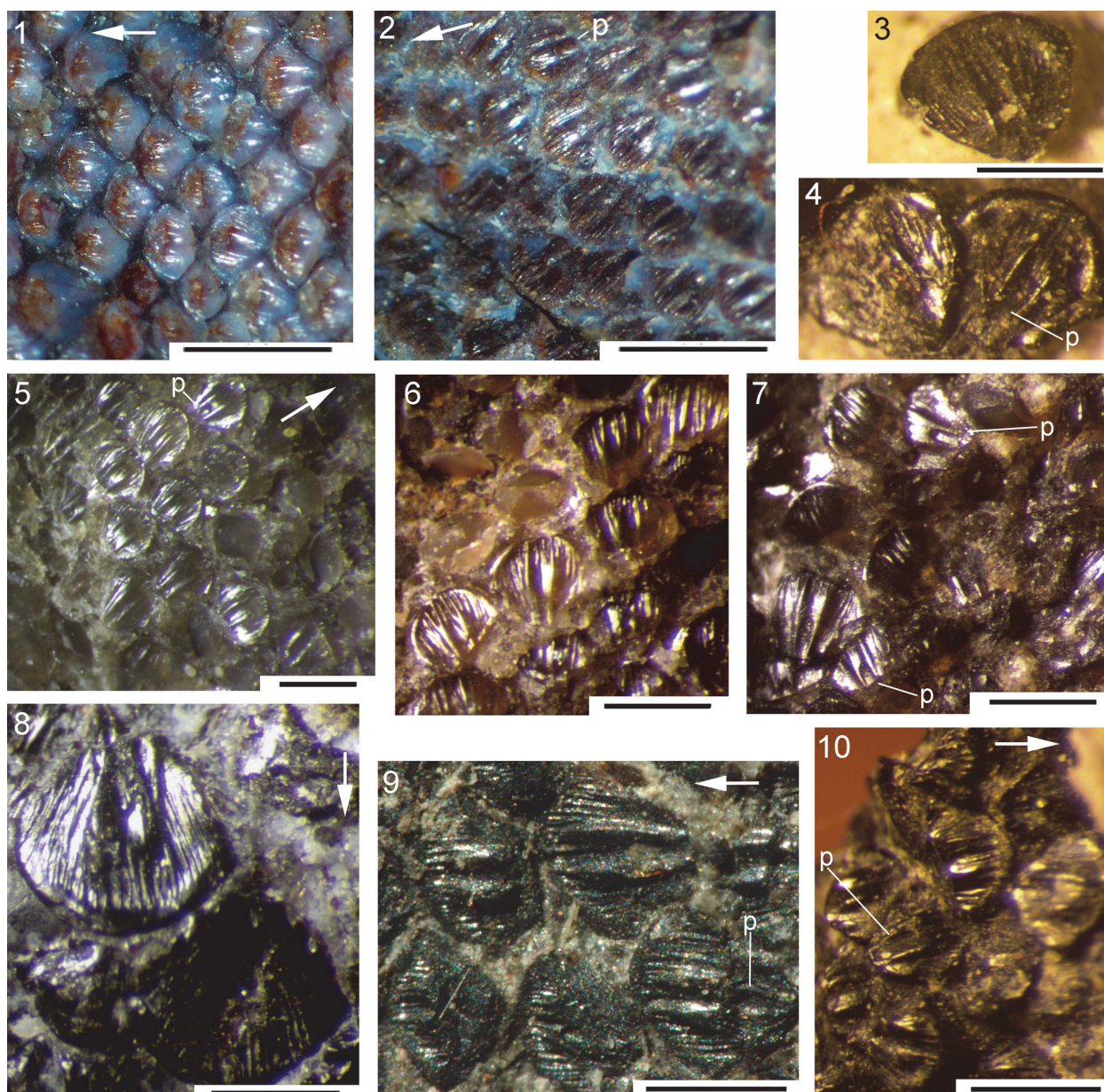


FIGURE 29. *Cheiracanthus latus* squamation, light microscope images. 1, 2, QMF60004 from Tynet Burn: 1, midflank scales; 2, caudal peduncle, scale impressions. 3, 4, NMS G.2018.28.26 from Tarrel Bay. 5-7, NMS G.2019.3.7 from Den of Findon, Banffshire 8, NMS G.2019.3.3 from Jessie Port. 9, NMS G.1870.14.145 from Cromarty. 10, NMS G.2019.9.17 from Geanies Point. Scale bars equal 0.5 mm. p, pit. Arrows indicate anterior.

this is a short D-shaped mineralised cartilage. The pulp cavity is open for about half the length of the spine. The pectoral spines have a smooth leading edge ridge, deep lateral groove, and thin longitudinal ridges along the side, usually best developed more proximally (Figure 26.4-5). A single row of pores opens out in the groove. They have a short insertion, and a strip lacking dentine extending along the upper side of the spine, where the scapulocoracoid abutted (Figure 26.6). Like the dorsal

spine, the anal and pelvic spines have a smooth leading edge ridge separated from the smooth sides by a deep groove (Figure 26.7).

The scapulocoracoid is formed of a dense lamellar bone around a central cavity (Figure 27.1-2). The histological structure of the fin spines is very similar to that of *C. munchisoni* and *C. grandispinus*, the main difference being that the lateral groove is not as deeply incised (Figures 27.3-9, 27.11-13, 28). The pectoral spines have a very thin

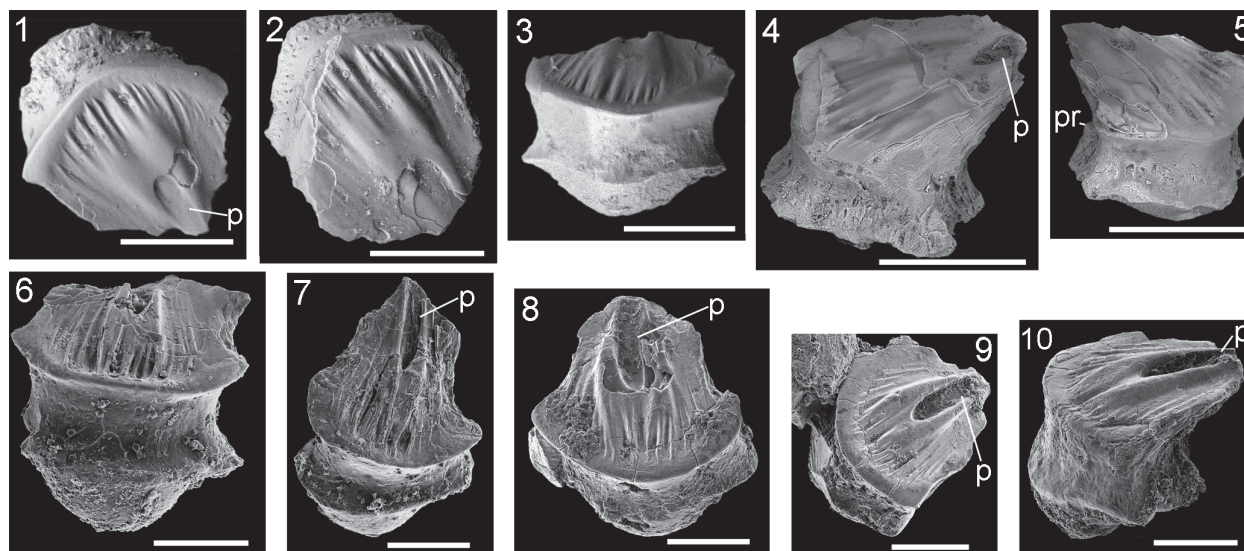


FIGURE 30. *Cheiracanthus latus* squamation, SEM images. 1-5, NMS G. 2019.3.7.21 from Den of Findon: 1, NMS G. 2019.3.7.21.2, crown view; 2, NMS G. 2019.3.7.21.5, crown view; 3, NMS G. 2019.3.7.21.13, anterior view; 4, NMS G. 2019.3.7.21.7, laterocrown view; 5, NMS G. 2019.3.7.21.14, laterocrown view. 6-7: NMS G.2019.14.9.2 from Geanies Point: 6, NMS G.2019.14.9.2.8, anterocrown view; 7, NMS G.2019.14.9.2.5, crown view. 8-10: NMS G.2019.14.4.2 from Hilton or Cadboll: 8, NMS G.2019.14.4.2.15, crown view; 9, NMS G.2019.14.4.2.5, crown view; 10, NMS G.2019.14.4.2.16, laterocrown view. Scale bars equal 0.2 mm. p, pit; pr, neck protuberance.

enameloid layer on the leading edge ridge and the 'shoulders', with most of the spine formed of osteodentine. Spines lack an accessory pulp canal. Pores leading from the vascular canals open out into the lateral groove (Figure 27.3-4, 27.13). Dentine tubules of the osteodentine layer are usually only visible near the surface of the anterior ridge (Figure 27.5), oriented perpendicular to the surface and running in to the more or less radially arranged vascular canals. The inner lamellar layer is very thin proximally, thickening distally (Figure 27.6, 27.9), and is penetrated by fine branching dentine tubules (Figure 27.10). The vascular canals and the central pulp cavity become almost closed by lamellar infilling towards the tip of the spine (Figure 27.6, 27.9-10), but canals still extend from the cavity through the dentine (Figure 27.7, 27.9-10). The inserted part of the spine lacks an outer enameloid cover and dentine tubules, and is composed of a vacuous osteodentine or bone (Figures 27.12, 28.1.12, 28.2.6). The thin longitudinal ridges on the sides of the spines are low, sharp-crested, and best visible in the proximal part of the spine (Figure 27.13-14).

Body scales: The mid-flank scales of *Cheiracanthus latus* range in size from 0.25 mm wide on small fish c. 130 mm long (Figure 29.1-2), c. 0.5 mm wide on medium sized fish (Figure 29.3-7), to 1.0 mm wide (Figure 29.8) on large fish. The scale crown has a marked smooth rim along the anterior

edge (Figures 29.4-8, 30.1-3, 30.5-10). The ornament over the rest of the crown comprises two prominent, broad ridges ("Groszrippen" of Gross, 1947, p. 125) extending back on either side of a median sulcus, and narrower, sharp-crested ridges on both sides of the median ridges extending back towards the serrated posterolateral edges of the crown (Figures 29.8, 30). A few short ridges are developed in the anterior part of the median sulcus, and an oval pit is developed in the posterior half of the scale within the sulcus (Figures 29.4, 29.5, 29.7-10, 30). The neck and base of the scales (Figure 30.3, 30.6, 30.10) closely resemble those of *C. murchisoni* in general profile and relative heights.

In most histological features the scales of *C. latus* resemble those of *C. murchisoni*, other than the development of a wide midline channel extending the length of the crown, which usually deepens to form an oval pit just posterior to the centre of the scale. The ridges extending back from the anterior edge are sharp-crested near this edge (Figure 31.1), becoming rounded more posteriorly (Figure 31.2), and often fading out past the posterior median pit (Figure 31.3-8). The crown is formed of up to 10 growth zones, which show that the wide central pit/channel was present at all stages from the embryonic/primordial scale (Figure 31.3-7). As in *C. murchisoni*, the primordial scale (c. 60 μ m long and 70 μ m wide) contains wide lacunae connected by short canals (Figure 31.8) with offshoots

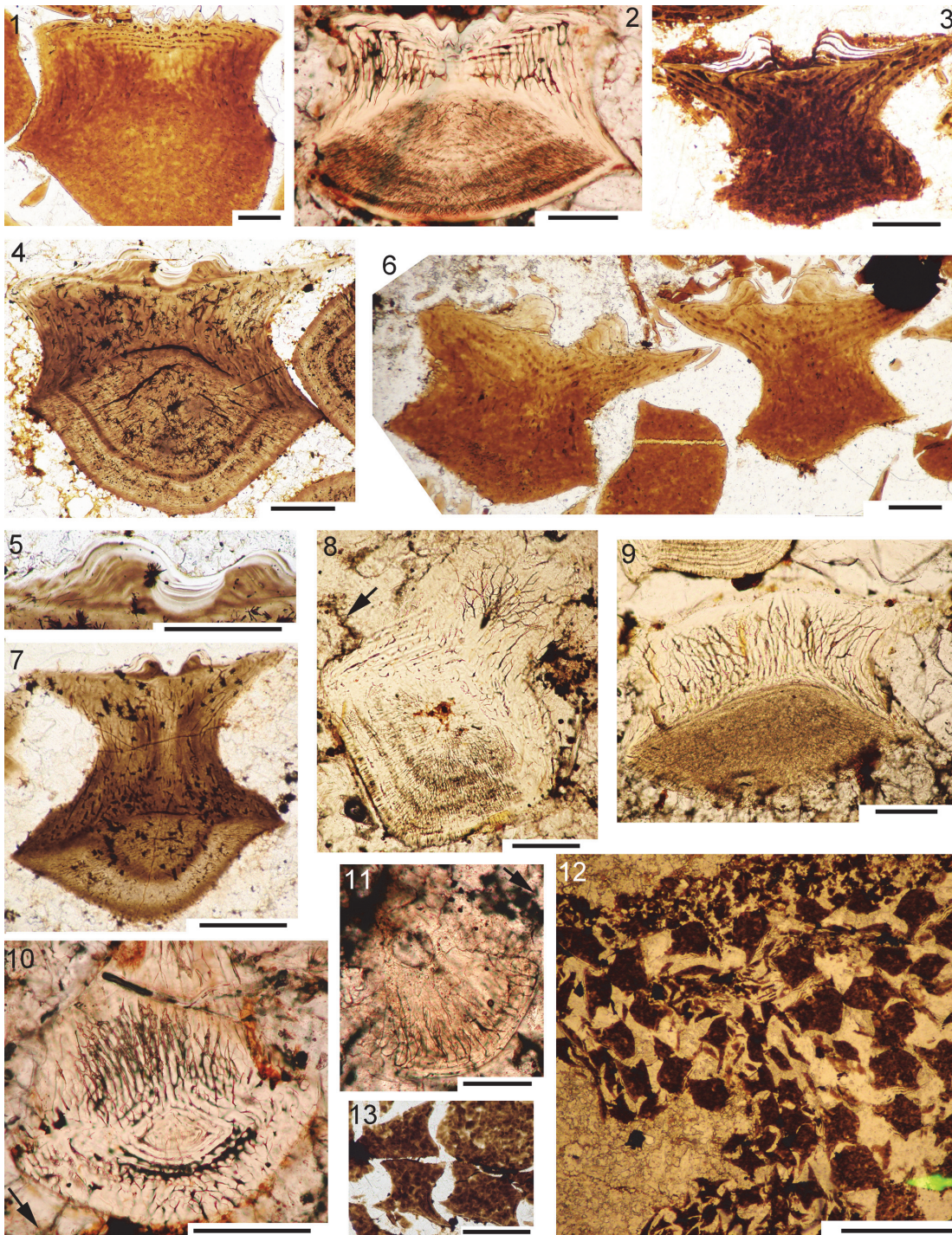


FIGURE 31. *Cheiracanthus latus* scale histology. 1, NMS G.2019.9.21.5, vertical transverse section, anterior half of scale. 2, NMS G.2019.9.19.2, vertical transverse section, anterior half of scale. 3, NMS G.2019.9.20.3, vertical transverse section, midscale. 4, 5, NMS G.2019.3.3.14, vertical transverse section, midscale, with closeup of central region. 6, NMS G.2019.9.21.3, vertical transverse sections of two scales, posterior half of scale. 7, NMS G.2019.3.3.12, vertical transverse section towards posterior end of scale. 8, NMS G.2019.3.7.6, subhorizontal section through anterior base and posterior crown. 9, NMS G.2019.3.7.6, vertical oblique section through posterior crown and base. 10, NMS G.2019.9.19.7, horizontal section low in crown. 11, NMS G.2019.9.22.5, horizontal section high in crown. 12, 13, NMS G.2019.9.23.7, section through fin web scales including tiny distal scales with a deep neck and flat base, closeup of distal fin web scales in 13. Scale bars equal 0.1 mm in 1-11,13, 0.5 mm in 12. Arrows indicate anterior.

extending down into the top of the basal cone. Each growth zone has its own system of anastomosing ascending canals, building an intricate network especially in the posterior side of the scales (Figure 31.7-9). The anterior areas of the crown growth zones are developed similarly to those of *C. purchisoni*, but differ in that the horizontal canals in the upper crown leading back from the semicircular ring canal are arranged much less regularly, and the lateral canals are better developed than the central canals (Figure 31.10, 31.11). This central area is delimited by two strongly developed horizontal canals, which extend further posteriorly than the other canals, in the larger ribs that flank the central pit. The horizontal canals are always situated in the grooves between crown ridges (Figure 31.1). In the posterior half of the crown, the ascending networks of canals gradually turn from a vertical into a more horizontal direction (Figure 31.8-10). The enameloid layers in the crown growth zones fill most of the depth of each zone in the ridges flanking the central pit, diminishing in depth laterally and disappear about halfway between the midline and the lateral edge. In the midline of the crown, enameloid layers are only developed anterior to the central channel and are completely lacking along most of the length (Figure 31.3-7). Fin web scales distal to the fin base differ markedly to the flank scales in their general shape, having a flat or concave base, deep neck, and crown plane that is concave both anteroposteriorly and side to side (Figure 31.12, 31.13).

Scale Comparisons

Cheiracanthus scales are common elements in microvertebrate assemblages from the Middle Devonian of the Baltic countries. Gross (1973) erected three new species, *C. brevicostatus*, *C. longicostatus*, and *C. splendens*, based on isolated scales mainly from the Eifelian Narva Formation, Estonia. The scale morphology of *C. longicostatus* Gross, 1973 appears identical to that of *C. latus*. Although Gross (1973, plate 28.16-20) differentiated the crown of *C. longicostatus* as relatively long and narrow, the figured scales do not corroborate this feature, as all have a width that is equal to or wider than the length, even when broken posterior ends are taken into account. One of the scales that Gross (1973, plate 28.12) assigned to his newly erected species *C. brevicostatus* should also be assigned to *C. latus*. At least some *C. brevicostatus* scales show features distinguishing them from other species – serrated posterior margins of crown growth zones and interconnections of hori-

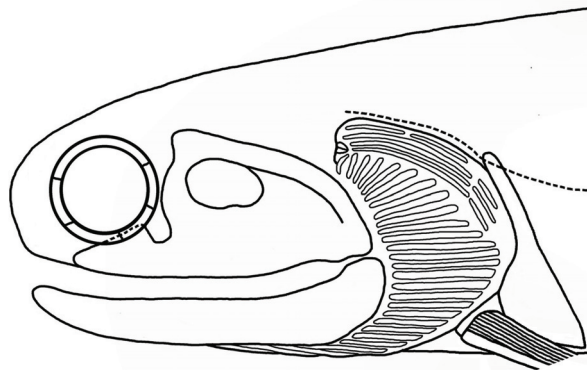


FIGURE 32. *Cheiracanthus latus* head and branchial region reconstruction.

zontal canals in the upper crown. The main feature determined by Gross (1973) to distinguish them from *C. purchisoni* is crown ridges of unequal width, but the crown on the holotype of *C. brevicostatus* (Gross, 1973, pl. 28.10) is similar to some *C. purchisoni* scale crowns (Figures 11, 12). We surmise that at least some of the records of *C. brevicostatus* from the Baltic countries are likely to be *C. purchisoni*, but are as yet unable to verify this determination. We have only identified one published illustration of a scale possibly assignable to *C. grandispinus* from the Baltic countries. Valiukevičius (1985, pl. 13.8) labelled the specimen from the Narva Formation as *Diplacanthus? carinatus*, but the crown closely resembles the distinctive *C. grandispinus* scale in Figure 20.10. Den Blaauwen et al. (2019) assigned the Narva Formation scale to *C. peachi*, as one of the scale morphotypes of the latter species (den Blaauwen et al., 2019, figure 7e-j) shows similarity to scales of *C. grandispinus*. Certainly in crown ornament, *C. peachi* most closely resembles *C. grandispinus*. *C. splendens* does not appear similar to scales on any of the Scottish *Cheiracanthus* specimens that we have examined. As we have noted, however, other newly identified Scottish cheiracanthid species are still to be described, one or more of which belong to taxa erected based on isolated scales from the Baltic countries.

Reconstruction of *Cheiracanthus*

The lateral reconstructions of *Cheiracanthus latus* (Figures 32, 33) closely follows Watson's (1937, figure 13) reconstruction except for details of the head, as described earlier, and the angle of the pectoral fin spine. The shallower angle of the pectoral fin spine is based on the alignment of the

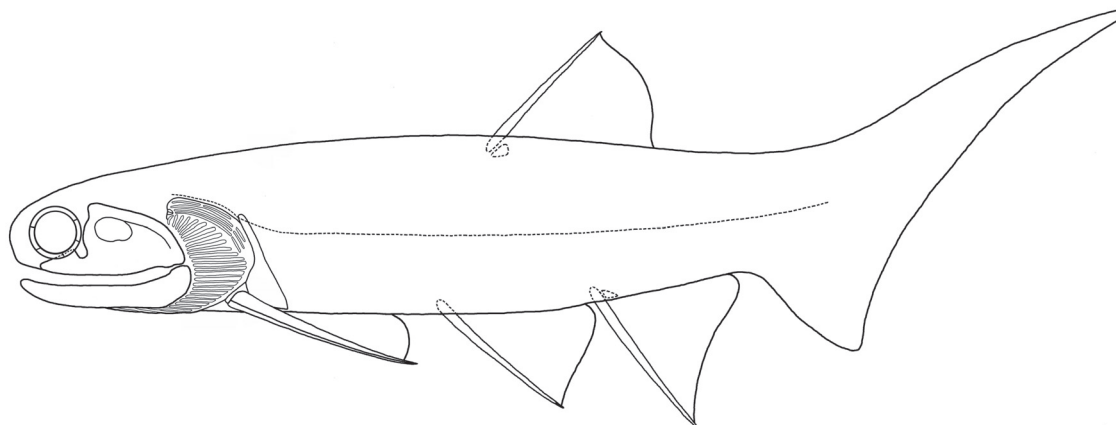


FIGURE 33. Reconstruction of a whole *Cheiracanthus latus* in lateral view.

upper edge of pectoral fin spine with the base of the scapula as described above. We speculate that these spines projected markedly laterally; when the fish were compressed during burial the spines were dislocated. All three species of *Cheiracanthus* described here have similar body shapes, with *C. latus* having a slightly larger and deeper caudal fin.

DISCUSSION

Although some aspects of the morphology of *C. murchisoni* and *C. latus* have been described previously (e.g., Miles, 1973), our work provides the first detailed description of *C. grandispinus*, showing that it is a valid species, characterised by the robustness of its fin spines and scapulocoracoid, and the distinctive fan-shaped ornament ridges on the scale crowns.

One of the features, which we describe for the first time in these three *Cheiracanthus* species, is the presence of denticles and gill bars in the branchial region, and tooth-like elements in the orobranchial region. The latter are smaller than those noted in the cheiracanthid *Homalacanthus concinnus* (e.g., Gagnier, 1996, figures 16, 18), and only rarely visible on articulated *Cheiracanthus* specimens, but are clearly seen in the serial sections, which show that they are formed of dentine like the ones in *H. concinnus*. It seems unlikely that they are typical gill rakers, as postulated by Zidek (1985), because they are only visible in the mouth region of articulated and sectioned *Cheiracanthus* specimens. It is perhaps surprising that the elements have been ignored since the original description of *C. latus*, but they are difficult to see in most specimens. We note that we have also identified a new cheiracanthid species in the Scot-

tish Middle Devonian, more similar to *Homalacanthus* than *Cheiracanthus*, which will be described in the near future.

We have also identified the bi-partite structure of the endoskeletal pectoral girdle, with a clear demarcation visible between the scapular and coracoid parts. Another notable observation relates to the D-shaped cartilages often mineralised at the base of the median fin spines (Figures 9.7, 9.8, 26.3): thin sections show that this cartilage extends into the pulp cavity of the fin spine as a thin lining (Figure 18.4, 18.6), reminiscent of the basal cartilages in both extant and extinct chondrichthyans (e.g., Maisey, 1979, figure 1B).

As well as the differences between the scales of the *Cheiracanthus* species, we have identified other morphological characters to distinguish between them: the scapular shaft is relatively more robust in *C. grandispinus* and expands dorsally, whereas it narrows in *C. murchisoni* and *C. latus*; the pectoral fin spine in *C. murchisoni* has thin longitudinal ridges ornamenting the sides, which are smooth in *C. grandispinus* and *C. latus*; the height of the leading edge ridge on fin spines of *C. grandispinus* is more than a third the total height of the spine, whereas it is a quarter or less the total height in *C. murchisoni* and *C. latus*; *C. latus* has a semi-lunar circumorbital plate above the orbit.

Our investigations have revealed new details of the structure of the endoskeletal tissues in *Cheiracanthus*, in particular the composition of the jaws and branchial arches. The endocranium was previously considered to be preserved as perichondral bone (e.g., Denison, 1979), but serial thin sections of all three species *C. murchisoni*, *C. grandispinus*, and *C. latus* (as well as the recently described new species *C. peachi*) have shown that

when the neurocranium and/or splanchnocranium is mineralised, it is mostly as a single layer of calcified cartilage (cc), often formed of contiguous blocks which are sub-rectangular in vertical section, as first noted by Ørvig (1951). In addition, some of the branchial bars are mineralised as a two-layered, consolidated calcified cartilage. We note that these two forms of calcified cartilage also occur in the same elements in the diplacanthiform *Diplacanthus crassisimus* (Dearden, 2019, figure 5.1). This co-occurrence could have interesting connotations from a phylogenetic perspective. Cheiracanthids are united with other acanthodiforms based primarily on acanthodids, mesacanthids, and cheiracanthids only having one dorsal fin spine. However, cheiracanthids differ from the other two families in having ornamented scale crowns, jaw cartilages mineralised as single units, lack of mandibular bones, and as we have shown here, an endoskeleton (other than the pectoral girdle) mineralised as calcified cartilage, not perichondral bone, and oral tooth-like elements. As the endoskeletal structure becomes better known and characterised in acanthodians and other stem chondrichthyans, their interrelationships will perhaps become clearer than cladistic analyses have so far deduced (e.g., Coates et al., 2018), with pro-

posed clades within the group generally poorly supported in those analyses.

We also note that some of the acanthodian species found in the Scottish Middle Devonian appear earlier in deposits further east. The taxa include *Cheiracanthus latus* (this work) and *Diplacanthus crassisimus* (Duff, 1842) – see Burrow et al. (2016) - which are both found in upper Emsian deposits of the Baltic region and Belarus. This stratigraphic distribution indicates that these species evolved in the eastern regions and migrated west to the Orcadian Basin of Scotland in the Eifelian. Newman et al. (2015, 2017) have noted that this westward migration of other classes of fish occurred in waves during the Middle Devonian, with very little endemism in the Orcadian Basin.

ACKNOWLEDGMENTS

The authors would like to thank T. Malvesy (Neuchâtel), E. Bernard (NHM), S. Walsh (NMS), B. Paton (previously NMS), M. Riley (SM), S. Johnston, R. Jones, Florian Witzmann (Berlin MN), T. Ziegler (NMV), C. Wellman (Sheffield University), B. Davidson, U. Michie†, J. Saxon†, for help with access and information on collections and specimens, localities, and interpreting stratigraphy. We also thank two anonymous reviewers for their advice and comments.

REFERENCES

- Agassiz, L. 1833-43. *Recherches sur les Poissons Fossiles*. Imprimerie de Petitpierre et Prince, Neuchâtel.
- Agassiz, L. 1844-45. *Monographie de Poissons Fossiles des Vieux Grès Rouges ou Système Dévonien (Old Red Sandstone) des Îles Britanniques et de Russie*. Imprimerie de Petitpierre et Prince, Neuchâtel.
- Albert, J.S., Johnson, D.M., and Knouft, J.H. 2009. Fossils provide better estimates of ancestral body size than do extant taxa in fishes. *Acta Zoologica* (Stockholm), 90(Suppl. 1):357-384. <https://doi.org/10.1111/j.1463-6395.2008.00364.x>
- Andrews, S.M. 1982. *The Discovery of Fossil Fishes in Scotland up to 1845 with Checklists of Agassiz's Figured Specimens*. Royal Scottish Museum, Edinburgh.
- Berg, L.S. 1940. Classification of fishes, both recent and fossil. *Trudy Instituta Zoologicheskikh Akademii Nauk*, 5(2):85-517.
- Beznosov, P. 2009. A redescription of the Early Carboniferous acanthodian *Acanthodes lopatini* Rohon, 1889. *Acta Zoologica (Stockholm)*, 90(suppl. 1):183-193.
- den Blaauwen, J.L., Newman, M.J., and Burrow, C.J. 2019. A new cheiracanthid acanthodian from the Middle Devonian (Givetian) Orcadian Basin of Scotland and its biostratigraphic and biogeographical significance. *Scottish Journal of Geology*, 55(2):166-177. <https://doi.org/10.1144/sjg2018-023>
- Blom, H., Carlsson, A., and Marshall, J.A.E. 2006. Vertebrate micro-remains from the Upper Devonian of East Greenland with comments on the Frasnian-Fammenian boundary. *Bulletin of the Geological Society of Denmark*, 53:39-46.

- Burrow, C.J. and den Blaauwen, J.L. in press. Endoskeletal tissues of acanthodians (stem Chondrichthyes). In Pradel, A., Janvier, P., and Denton, J.S.S. (eds.), *Ancient Fishes and Their Living Relatives: a Tribute to John G. Maisey*. Verlag Dr Friedrich Pfeil, Munich.
- Burrow, C., den Blaauwen, J., Newman, M., and Davidson, R. 2016. The diplacanthid fishes (Acanthodii, Diplacanthiformes, Diplacanthidae) from the Middle Devonian of Scotland. *Palaeontologia Electronica*, 19.1.10A:1–83. <https://doi.org/10.26879/601>
 palaeo-electronica.org/content/2016/1398-scottish-diplacanthid-fishes
- Burrow, C.J., Newman, M.J., Davidson, R.G., and den Blaauwen, J.L. 2011. Sclerotic plates or circumorbital bones in early jawed fishes? *Palaeontology*, 54(1):207-214. <https://doi.org/10.1111/j.1475-4983.2010.01003.x>
- Burrow, C.J., Newman, M.J., and den Blaauwen, J.L. 2020. First evidence of a functional spiracle in stem chondrichthyan acanthodians, with the oldest known elastic cartilage. *Journal of Anatomy*. <https://doi.org/10.1111/JOA.13170>
- Burrow, C.J. and Turner, S. 2010. Reassessment of “*Protodus*” *scoticus* from the Early Devonian of Scotland, p. 123-144. In Elliott, D.K., Maisey, J.G., Yu, X., and Miao, D. (eds.), *Morphology, Phylogeny and Paleobiogeography of Fossil Fishes*. Verlag Dr Friedrich Pfeil, Munich.
- Burrow, C.J. and Young, G.C. 2005. The acanthodian fauna of the Craven Peaks Beds (Early to Middle Devonian), western Queensland. *Memoirs of the Queensland Museum*, 51(1):3-25.
- Coates, M.I., Finarelli, J.A., Sansom, I.J., Andreev, P.S., Criswell, K.E., Tietjen, K., Rivers, M.L., and La Riviere, P.J. 2018. An early chondrichthyan and the evolutionary assembly of a shark body plan. *Proceedings of the Royal Society B: Biological Sciences*, 285:1-10. <https://doi.org/10.1098/rspb.2017.2418>
- Dean, B. 1907. Notes on acanthodian sharks. *American Journal of Anatomy*, 7:209-222.
- Davidson, R.G. and Trewin, N.H. 2005. Unusual preservation of the internal organs of acanthodian and actinopterygian fish in the Middle Devonian of Scotland. *Scottish Journal of Geology*, 41:129-134.
- Dearden, R. 2019. *The Anatomy and Evolution of "Acanthodian" Stem-chondrichthyans*. Unpublished PhD thesis, Department of the Life Sciences, Imperial College, London, UK.
- den Blaauwen, J.L., Newman, M.J., and Burrow, C.J. 2019. A new cheiracanthid acanthodian from the Middle Devonian (Givetian) Orcadian Basin of Scotland and its biostratigraphic and biogeographical significance. *Scottish Journal of Geology*, 55(2):166-177. <https://doi.org/10.1144/sjg2018-023>
- Denison, R.H. 1979. Acanthodii. In Schultze, H.-P. (ed.), *Handbook of Paleoichthyology, Part 5*. Gustav Fischer Verlag, Stuttgart and New York.
- Dineley, D.L. and Metcalf, S.J. (eds.). 1999. *Fossil Fishes of Great Britain*. Geological Conservation Review, 16. Joint Nature Conservation Committee Peterborough, UK.
- Duff, P. 1842. *Sketch of the Geology of Moray*. Forsyth and Young, Elgin.
- Egerton, P. de M.G. 1860. Palichthyologic notes, n. 12, remarks on the nomenclature of Devonian fishes. *Quarterly Journal of the Geological Society*, 16:119-136.
- Egerton, P. de M.G. 1861. British fossils, p. 51-75. In Huxley, T.H. (ed.), *Preliminary Essay Upon the Systematic Arrangement of the Fishes of the Devonian Epoch, Figures and Descriptions Illustrative of British Organic Remains*. Memoirs of the Geological Survey, U.K. (Decade 10).
- Gagnier, P.-Y. 1996. Acanthodii, p. 149-164. In Schultze, H.-P. and Cloutier, R. (eds.), *Devonian Fishes and Plants of Miguasha, Quebec, Canada*. Pfeil, Munich.
- Gillis, J.A., Dahn, R.D., and Shubin, N.H. 2009. Chondrogenesis and homology of the visceral skeleton in the little skate, *Leucoraja erinacea* (Chondrichthyes: Batoidea). *Journal of Morphology*, 270(5):628-43. <https://doi.org/10.1002/jmor.10710>
- Gillis, J.A. and Tidswell, O.R.A. 2017. The origin of vertebrate gills. *Current Biology*, 27(5):729-732. <https://doi.org/10.1016/j.cub.2017.01.022>
- Glinskiy, V.N. and Pinakhina, D.V. 2018. New data on psammosteid heterostracans (Pteraspodomorpha) and acanthodians (Acanthodii) from the Pärnu Regional Stage (Lower Eifelian, Middle Devonian) of Estonia. *Estonian Journal of Earth Sciences*, 67(1):76-87. <https://doi.org/10.3176/earth.2018.05>
- Gross, W. 1947. Die Agnathen und Acanthodier des obersilurischen Beyrichienkalks. *Palaeontographica A*, 96:91-161.
- Gross, W. 1973. Kleinschuppen, Flossenstacheln und Zähne von Fischen aus europäischen und nordamerikanischen Bonebeds des Devons. *Palaeontographica A*, 142:51-155.

- Hanke, G.F. and Wilson, M.V.H. 2004. New teleostome fishes and acanthodian systematics, p. 189-216. In Arratia, G., Wilson, M.V.H., and Cloutier, R. (eds.), *Recent Advances in the Origin and Early Radiation of Vertebrates*. Verlag Dr. Friedrich Pfeil, Munich.
- Ivanov, A. and Marss, T. 2014. New data on *Karksiodus* (Chondrichthyes) from the Main Devonian Field (East European Platform). *Estonian Journal of Earth Sciences*, 63(4):156-165. <https://doi.org/10.3176/earth.2014.14>
- Jeannet, A. 1927. Les poissons fossiles originaux conservés à l'institut de géologie de l'université de Neuchâtel. *Bulletin de la Société Neuchâteloise des Sciences Naturelles*, 52:102-124.
- Maisey, J.G. 1979. Finspine morphogenesis in squalid and heterodontid sharks. *Zoological Journal of the Linnean Society*, 66:161-183.
- M'Coy, F. 1848. On some new Ichthyolites from the Scotch Old Red Sandstone. *The Annals and Magazine of Natural History*, Second Series 11:297-312.
- M'Coy, F. 1855. *Description of the British Palaeozoic Fossils in the Geological Museum of the University of Cambridge*. John W. Parker and Son, London.
- Miles, R.S. 1966. The acanthodian fishes of the Devonian Plattenkalk of the Paffrath Trough in the Rhineland. *Arkiv för Zoologi*, 18(9):147-194.
- Miles, R.S. 1970. Remarks on the vertebral column and caudal fin of acanthodian fishes. *Lethaia*, 3:343-362.
- Miles, R.S. 1973. Articulated acanthodian fishes from the Old Red Sandstone of England, with a review of the structure and evolution of the acanthodian shoulder-girdle. *Bulletin of the British Museum (Natural History), Geology*, 24(2):113-213.
- Miller, H. 1841. *Old Red Sandstone or New Walks in an Old Field* (first edition). John Johnstone, Edinburgh.
- Miller, H. 1847. *Old Red Sandstone or New Walks in an Old Field* (third edition). John Johnstone, Edinburgh.
- Nelson, G.J. 1968. Gill-arches in *Acanthodes*, p. 129-143. In Ørvig, T. (ed.), *Current Problems of Lower Vertebrate Phylogeny*. Almqvist & Wiksell, Stockholm.
- Newman, M.J., den Blaauwen, J.L., and Tuuling, T. 2017. Middle Devonian coccosteid (Arthrodira, Placodermi) biostratigraphy of Scotland and Estonia. *Scottish Journal of Geology*, 53(2):63-69. <https://doi.org/10.1144/sjg-2016-012>
- Newman, M.J., Burrow, C.J., and Blaauwen, J.L. den 2019. The Givetian vertebrate fauna from the Fiskekløfta Member (Mimerdalen Subgroup), Svalbard. Part I. Stratigraphic and faunal review. Part II. Acanthodii. *Norwegian Journal of Geology*, 99(1):1-16. <https://doi.org/10.17850/njg99-1-01>
- Newman, M.J. and Dean, M.T. 2005. A biostratigraphical framework for geological correlation of the Middle Devonian strata in the Moray-Ness Basin Project area. British Geological Survey Internal Report IR/05/160.
- Newman, M.J., Mark-Kurik, E., den Blaauwen, J.L., and Zupinš, I. 2015. Scottish Middle Devonian fishes in Estonia. *Scottish Journal of Geology*, 51(2):141-147. <https://doi.org/10.1144/sjg2014-006>
- Ørvig, T. 1951. Histologic studies of Placoderms and fossil Elasmobranchs. *Archiv för Zoologi*, 2(2):321-454.
- Owen, R. 1846. *Lectures on the Comparative Anatomy and Physiology of the Vertebrate Animals Delivered at the Royal College of Surgeons, England in 1844 and 1846. Part I, Fishes*. Longman, Brown, Green and Longmans, London.
- Paton, R.L. 1976. A catalogue of fossil vertebrates in the Royal Scottish Museum, Edinburgh. Part Five. Acanthodii. *Royal Scottish Museum Information Series, Geology*, 6:1-40.
- Pinakhina, D.V. 2018. A new cheiracanthid acanthodian species from the Aruküla Regional Stage (Middle Devonian, Givetian) of the Eastern Main Devonian Field. *Paleontological Journal*, 52(1):42-48. <https://doi.org/10.1134/S0031030118010112>
- Pinakhina, D.V. and Marss, T. 2018. The Middle Devonian acanthodian assemblage of the Karksi outcrop in Estonia. *Estonian Journal of Earth Sciences*, 67(1):96-111. <https://doi.org/10.3176/earth.2018.07>
- Plax, D.P. 2015. Stratigraphic ichthyofauna assemblages of the Devonian deposits in the east and southeast of Belarus. *Lithosphaera*, 42(1):20-44.
- Plax, D.P. and Zaika, Y.V. 2018. On the Sargaevo Deposits (Frasnian, Upper Devonian) of the Latvian Saddle outcropping within the Saryanka River Basin (Belarus). *Lithosphaera*, 2:54-82.

- Retallack, G.J. 2011. Exceptional fossil preservation during CO2 greenhouse crises? *Palaeogeography, Palaeoclimatology, Palaeoecology*, 307(1/4):59-74. <https://doi.org/10.1016/j.palaeo.2011.04.023>
- Russell, L.S. 1951. Acanthodians of the Upper Devonian Escuminac Formation, Maguasha, Quebec. *Annals and Magazine of Natural History*, ser. 12, 4:401-407.
- Sallan, L.C. and Coates, M.I. 2010. End-Devonian extinction and a bottleneck in the early evolution of modern jawed vertebrates. *Proceedings of the National Academy of Sciences of the United States of America*, 107, SI Appendix. <https://doi.org/10.1073/pnas.0914000107>
- Schultze, H.P. 1972. *Homalacanthus*, ein oberdevonischer Acanthodier mit Haifisch-ähnlichen Zähnen. *Neue Jahrbuch für Geologie und Paläontologie Monatsheft*, 1972:312-317.
- Taylor, P.D. and O'Dea, A. 2014. *A History of Life in 100 Fossils*. Natural History Museum, London.
- Traquair, R.H. 1888. Notes on the nomenclature of the fishes of the Old Red Sandstone of Great Britain. *The Geological Magazine*, Decade III, 5:507-517.
- Traquair, R.H. 1893. Notes on the Devonian fishes of Campbelltown and Scaumenac Bay in Canada. Part 1. *Proceedings of the Royal Physical Society of Edinburgh*, 12:111-118.
- Traquair, R.H. 1895. The extinct vertebrate animals of the Moray Firth area, p. 235-285. In Harvie-Brown, J.A. and Buckley, T.E. (eds.), *A Vertebrate Fauna of the Moray Firth Basin, Volume 2*. D. Douglas, Edinburgh.
- Valiukevičius, J.J. 1985. *Acanthodians from the Narva Regional Stage of the Main Devonian Field*. Mokslas, Vilnius. (In Russian with English summary)
- Valiukevičius, J.J. 1988. New acanthodians from the Middle Devonian of the Baltic and Byelorussia. *Palaeontological Journal*, 2:80-86.
- Valiukevičius, J.J. 2000. Acanthodian biostratigraphy and interregional correlations of the Devonian of the Baltic States, Belarus, Ukraine and Russia. *Courier Forschungsinstitut Senckenberg*, 223:271-289.
- Valiukevičius, J. 2002. Early and Middle Devonian acanthodian associations of Lithuania with respect to the lithofacies. *Litosfera*, 6:30-39.
- Valiukevičius, J.J. and Karatajūtė-Talimaa, V.N. 1986. Acanthodian scale assemblage from the base of the Middle Devonian of the Baltic and Byelorussia, p. 110-122 (in Russian). In Brangulis, A.P. (ed.), *Biofacies and Fauna of the Silurian and Devonian Basins of the Baltic region*. Zinatne, Riga.
- Valiukevičius, J., Talimaa, V., and Kruczek, S. 1995. Complexes of vertebrate microremains and correlation of terrigenous Devonian deposits of Belarus' and adjacent territories. *Ichthyolith Issues Special Publication*, 1:53-59.
- Watson, D.M.S. 1935. Fossil fishes of the Orcadian Old Red Sandstone, p. 157-169. In Wilson, G.V., Knox, J., Jones, R.C.B., and Stephens, J.V. (eds.), *The Geology of the Orkneys*. His Majesty's Stationery Office, Edinburgh.
- Watson, D.M.S. 1937. The acanthodian fishes. *Philosophical Transactions of the Royal Society (B)*, 228:49-146.
- White, E.I. 1968. Devonian fishes of the Mawson-Mulock area, Victoria Land, Antarctica. *Trans-Antarctic Expedition 1955-1958, Scientific Reports, Geology*, 16:1-26.
- Whiteaves, J. 1887. Illustrations of the fossil fishes of the Devonian rocks of Canada. *Proceedings and Transactions of the Royal Society of Canada*, 4(4):101-110.
- Woodward, A.S. 1891. *Catalogue of the Fossil Fishes in the British Museum (Natural History). Part II*. British Museum (Natural History), London.
- Woodward, A.S. and Sherborn, C.D. 1890. *A Catalogue of British Fossil Vertebrata*. Dulau and Co, London.
- Young, G.C., and Burrow, C.J. 2004. Diplacanthid acanthodians from the Aztec Siltstone (late Middle Devonian) of southern Victoria Land, Antarctica. *Fossils and Strata*, 50:23-43.
- Young, V.T. 1995. Micro-remains from Early and Middle Devonian acanthodian fishes from the U.K. and their biostratigraphic possibilities. *Ichthyolith Issues Special Publication*, 1:65-68.
- Young, V.T. 1997. Early Palaeozoic acanthodians in the collection of the Natural History Museum, London. *Ichthyolith Issues Special Publication*, 3:46-50.
- Zidek, J. 1976. Kansas Hamilton Quarry (Upper Pennsylvanian) *Acanthodes*, with remarks on the previously reported North American occurrences of the genus. *The University of Kansas Paleontological Contributions*, Paper 83:1-41.
- Zidek, J. 1985. Growth in *Acanthodes* (Acanthodii: Pisces) data and implications. *Paläontologische Zeitschrift*, 59:147-166.